UNIVERZITA PALACKÉHO V OLOMOUCI

Přírodovědecká fakulta

Katedra biotechnologií

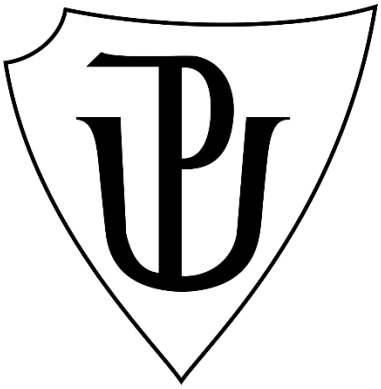

3D sféroidní kultury lidské buněčné linie pro modelování onemocnění a objevování léků

DIPLOMOVÁ PRÁCE

Autor:	**Bc. Eliška Šimíčková**
Studijní program:	N0512A130007 Biotechnologie a genové inženýrství
Specializace:	Biotechnologie a genové inženýrství
Forma studia:	Prezenční
Vedoucí práce:	**M.Sc Viswanath Das, Ph.D.**
Rok:	2025

PALACKÝ UNIVERSITY IN OLOMOUC

Faculty of Science

Department of biotechnology

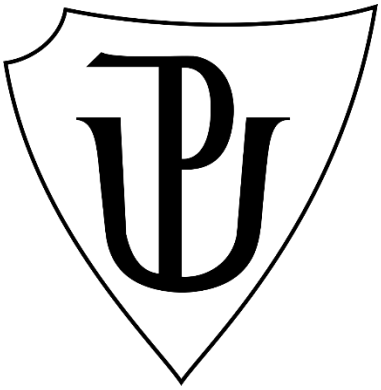

3D culture of human cell lines for disease modeling and drug discovery

DIPLOMA THESIS

Author:	**Bc. Eliška Šimíčková**
Study program:	N0512A130007 Biotechnology and gene engineering
Branch of study:	Biotechnology and gene engineering
Form of study:	Full time
Supervisor:	**M.Sc Viswanath Das, Ph.D.**
Year:	2025

Prohlašuji, že jsem diplomovou práci vypracovala samostatně s vyznačením všech použitých pramenů a spoluautorství. Souhlasím se zveřejněním diplmové práce podle zákona č. 111/1998 Sb., o vysokých školách, ve znění pozdějších předpisů. Byla jsem seznámena s tím, že se na moji práci vztahují práva a povinnosti vyplývající ze zákona č. 121/2000 Sb., autorský zákon, ve znění pozdějších předpisů.

V Olomouci dne ....……

Podpis studenta

I declare that I have prepared the diploma thesis independently, indicating all sources used and co-authorship. I agree with the publication of the diploma thesis according to Act no. 111/1998 Coll., On Higher Education, as amended. I have been informed that my thesis is subject to the rights and obligations arising from Act No. 121/2000 Coll., Copyright Act, as amended.

In Olomouc ....

Student's signature

Acknowledgments:

First and foremost, I would like to express my gratitude to my supervisor, M.Sc Viswanath Das, Ph.D, for his time, dedication, support, and valuable advice during the preparation of my thesis. I would also like to extend my sincere thanks to all members of the Institute of Molecular and Translational Medicine, with whom I had the opportunity to collaborate, especially Mgr. Anna Janošťáková and Mgr. Ihor Kozlov for their assistance and valuable guidance during my laboratory work. Finally, I would like to express my heartfelt thanks to my husband Martin and my entire family, who supported me throughout this journey — without them, it would not have been possible.

This work was supported in parts by the infrastructural projects (CZ-OPENSCREEN – LM2023052; EATRIS-CZ – LM2023053; Czech-BioImaging – LM2023050; LM2018129), the project National Institute for Cancer Research (Program EXCELES, ID Project No. LX22NPO5102, Funded by the European Union - Next Generation EU), the project SALVAGE (registration number: CZ.02.01.01/00/22_008/0004644, supported by OP JAK, with co-financing from the EU and the State Budget) from the Ministry of Education, Youth and Sports of the Czech Republic (MEYS), and the project TN02000109 (Personalized Medicine: From Translational Research into Biomedical Applications is co-financed with the state support of the Technology Agency of the Czech Republic as part of the National Centers of Competence Program).

Bibliografická identifikace

Jméno a příjmení autora	Bc. Eliška Šimíčková
Název práce	3D sferoidní kultury lidské buněčné linie pro modelování nemocí a objevování léčiv
Typ práce	Diplomová
Pracoviště	Ústav molekulární a translační medicíny
Vedoucí práce	M.Sc Viswanath Das, Ph.D.
Rok obhajoby práce	2025

Abstrakt

Sféroidy představují 3D model vhodný pro studium interakcí mezi buňkami a testování účinků léčiv, který poskytuje fyziologicky relevantnější prostředí ve srovnání s tradičními 2D kulturami. Cílem této práce bylo vytvořit monokultury sféroidů z buněčné linie kolorektálního karcinomu HCT116 (a jejích mutantních variant) a vyhodnotit účinek lymfocytů (kontrolní lymfocyty, CuET-ošetřené lymfocyty, IL-2-ošetřené lymfocyty) na růst a životaschopnost sféroidů pomocí fluorescenční mikroskopie a měření ATP pomocí kitu CellTiter-Glo. Dále bylo cílem studie vytvořit kokultury sféroidů z buněčné linie HCT116 a normální linie kolonických fibroblastů CCD18-Co a posoudit synergický účinek vybraných kombinací léčiv na molekulární úrovni pomocí western blot analýzy. Výsledky ukázaly, že IL-2-ošetřené lymfocyty vykazovaly nejvyšší cytotoxicitu, zejména u buněčných linií s funkčním nebo částečně funkčním p53. Nejefektivnější kombinací léčiv byl irinotekan:cisplatina v poměru 4:1, následovaný kombinací 5-fluorouracil:cisplatina v poměru 1:1. Metoda tvorby sféroidů na agarózou potažených destičkách, spolu s optimalizovanými analytickými technikami, poskytuje slibnou platformu pro vývoj nových terapeutických přístupů.

Klíčové slova	HCT116 buněčná linie, CCD18-Co buněčná linie, kokultury, sferoidy, lymfocyty, fluorescenční mikroskopie, CellTiterGlo, agarózou pokryté destičky, synergický efekt
Počet stran	69
Počet příloh	0
Jazyk	Anglický

Bibliographical identification

Author's first name and surname	Bc. Eliška Šimíčková
Title	3D culture of human cell lines for disease modeling and drug discovery
Type of thesis	Diploma
Department	IMTM
Supervisor	M.Sc Viswanath Das, Ph.D.
The year of presentation	2025

Abstract

Spheroids represent a 3D model suitable for studying cell interactions and testing drug effects, providing a more physiologically relevant environment compared to traditional 2D cultures. The aim of this work was to create monocultures of spheroids from the colorectal carcinoma cell line HCT116 (and its mutant variants) and evaluate the effect of lymphocytes (control lymphocytes, CuET-treated lymphocytes, IL-2-treated lymphocytes) on spheroid growth and viability using fluorescence microscopy and ATP measurement with the CellTiter-Glo kit. Additionally, the study aimed to establish cocultures of spheroids from the HCT116 cell line and the normal colon fibroblast line CCD18-Co and assess the synergistic effect of selected drug combinations at the molecular level using western blot analysis. The results showed that IL-2-treated lymphocytes exhibited the highest cytotoxicity, particularly in cell lines with functional or partially functional p53. The most effective drug combination was irinotecan:cisplatin at a ratio of 4:1, followed by 5-fluorouracil:cisplatin at a ratio of 1:1. The method of spheroid formation on agarose-coated plates, along with optimized analytical techniques, provides a promising platform for the development of new therapeutic approaches.

Keywords	HCT116 cell line, CCD18-Co cell line, co-cultures, spheroids, lymphocytes, fluorescence microscopy, CellTiterGlo, agarose-coated plates, synergistic effect
No. of pages	69
No. of attachments	0
Language	English

Contents

Aims

The aim of this study is to utilize 3D spheroid cultures for modeling the tumor microenvironment and evaluating the effects of lymphocytes and drug combinations on colorectal cancer cells. The theoretical part aims to describe types of 3D cell cultures, differences in the use of 2D and 3D cultures, methods of spheroid formation, and the description of spheroids as a physiological model. In experimental part, spheroids will be generated using established protocols with HCT116 colorectal cancer cells and CCD18-Co normal colon fibroblasts, including co-culture models to better mimic cell interactions. The effects of control, copper diethyldithiocarbamate (CuET)-treated, and interleukin 2 (IL-2)-treated lymphocytes will be assessed using fluorescence microscopy and CellTiter-Glo®. Molecular changes following drug treatment will be analyzed by Western blot and synergy effect will be examined. This approach aims to provide insights into cellular responses in 3D environments.

1 Introduction

One of the current priorities of biomedical research is to search for new experimental models and strategies suitable for high-throughput screening and routine use in clinical laboratories. Traditional 2D cell cultures, although used for a long time, have proven insufficient in many studies because they cannot fully imitate complex physiological conditions in the organism. These conditions play a crucial role, for example, in the response to drug treatment or in investigating the mechanisms of cellular reactions.

Spheroids appear to be a promising alternative in this context, which, thanks to their 3D structure, allow for much more realistic monitoring of cell interactions, gene expression, and signaling pathways compared to traditional 2D cultures. Although spheroids are increasingly used, their wider application in practice is still limited by some technical challenges requiring optimizing laboratory methods.

This diploma thesis focuses on using spheroids to evaluate the effects of stimulated lymphocytes and test combinations of cytostatics to verify their synergistic effect. The aim of the work is to assess the effectiveness of different types of lymphocytes (control, CuET-stimulated lymphocytes, and IL-2-stimulated lymphocytes) on the growth and viability of spheroids and to analyze key cell markers (Ac-α-tubulin, p21) when testing the synergistic effect of drugs.

The results of this work can contribute to the optimization of laboratory methods and provide new knowledge that can be used in developing new therapeutic approaches, especially in the field of personalized medicine.

2 Current state of the topic

2.1 3D cultures

The cultivation of cell cultures has its roots in the early 20th century. The first cultured cells were nerve cells from the spinal cord of amphibians, in 1907 by American biologist Ross Granville Harrison. The first human *in vitro* cultured cell line, HeLa, originated from cervical cancer in a patient named Henrietta Lacks and was cultivated using the roller-tube technique (Yao & Asayama, 2017).

Although 2D cell cultures remain quite popular in biomedical sciences, they have significant limitations. However, these limitations can be overcome by transitioning to 3D cell line cultivation. One of these 3D cell lines is organoids and spheroids.

American scientist Dr. Sutherland cultivated so-called multicellular spheroids (MCS) in the 1970s. He used these cell aggregates to study the organization of tumor cells. As one of the first scientists, he provided a realistic model of tumor cell behavior and demonstrated how their microenvironment influences them. Research by his team further described the so-called contact effect, a phenomenon in which multicellular spheroids exhibit increased resistance to the effects of radiation and cytostatic (Sutherland, 1988).

Spheroid and multicellular spheroid models function based on the ability of cells to adhere to one another while preventing them from attaching to the plastic surfaces of culture flasks. These models have become very popular in recent years because they mimic tissue and tumor environments more effectively than 2D cell lines. Spheroids can be derived from various cells, such as cancer cells, neurons, hepatocytes, or fibroblasts. Their microenvironment closely resembles the physiological conditions of tumors and tissues, accurately mimicking architecture and facilitating similar intercellular interactions. The nature of spheroids allows for the formation of nutrient and oxygen gradients that influence cell metabolism and gene expression, enabling us to observe physiological responses (Lee et al., 2023).

Organoids can be characterized as cell clusters that can simulate the structure and function of real organs. They can be derived from three main types of tissues. The first type of organoids is those derived from pluripotent stem cells. These cells can differentiate into various kinds of cells, a broad spectrum of organoids. The second type is organoids derived from adult stem cells. These cells have a more limited ability to

differentiate, meaning they can only create specific types of cells. The third type includes organoids formed from somatic cells, which are not stem cells and have specific bodily functions. These organoids are used to model various physiological and pathological conditions. Organoids are generally complex in morphology, exhibit organogenesis properties, and can mimic organ development *in vitro* (Calà et al., 2023).

The difference between spheroids and organoids can be summarized like this: spheroids are aggregated cells forming a 3D structure, whereas organoids, due to their specific origin, more closely mimic the structure and function of a particular organ. Although spheroids do not directly mimic organ environments, they offer many advantages in research. They are popular mainly due to the simplicity of preparation, which is quicker than organoids. They are also less costly, highly variable, and demonstrate more excellent reproducibility (Sakalem et al., 2020).

Organoids and spheroids offer numerous advantages over the classical cultivation of adherent cells in flasks. These 3D models provide biochemical and integrative mechanisms like those occurring under physiological conditions. They enable the observation of cell responses to drugs, mimic tumor diseases, and allow the study of host-pathogen interactions. Their use in studying various human diseases allows us to better understand cell behavior without subjecting animals to unnecessary suffering. In this way, we can obtain valuable information about the pathogenesis of diseases, drug testing, and the development of new therapeutic approaches, contributing to more ethical and sustainable research (Lee et al., 2023).

2.2 Spheroids

As mentioned in Chapter 2.1, spheroids are cellular aggregates cultured in an environment that prevents them from attaching to a flat surface. Typically, these aggregates form in three stages. The first stage involves dispersed cells clustering with the aid of extracellular matrix fibers containing the arginylglycylaspartic acid motif. This motif enables binding to integrins, transmembrane adhesion molecules that also activate focal adhesion kinase (FAK), a cytoplasmic tyrosine kinase. FAK plays a key role in cell growth, migration, and adhesion by promoting the rearrangement of actin filaments and microtubules.

This integrin binding increases the expression of transmembrane proteins called cadherins. In the second stage, cadherins accumulate on the cell membrane surface. The final stage of spheroid formation involves the formation of cadherin-cadherin bonds, creating tight cell-to-cell connections and leading to the cohesive spheroid structure. Both the actin cytoskeleton and microtubules are critical in spheroid formation, as they support cell adhesion and aggregation (Lin & Chang, 2008).

The size of spheroids is determined by the number of cells that form them. When 4,000–8,000 cells are used per spheroid, the size reaches approximately 400–700 micrometers, with the optimal size being around 500 micrometers.

The size of spheroids also influences their morphology, which typically consists of three layers described in Fig. 1. The first, the outer proliferative layer, contains metabolically active cells due to easy access to nutrients and oxygen. The middle layer, the quiescent intermediate layer, comprises cells with adequate oxygen and nutrient supply, but these cells are not as metabolically active as those in the proliferative zone. In the very core of the spheroid, necrotic cells accumulate due to a lack of nutrients and the buildup of waste products. This environment is highly hypoxic, and in spheroids formed from tumor cells, it effectively mimics the tumor microenvironment (Alzeeb et al., 2020).

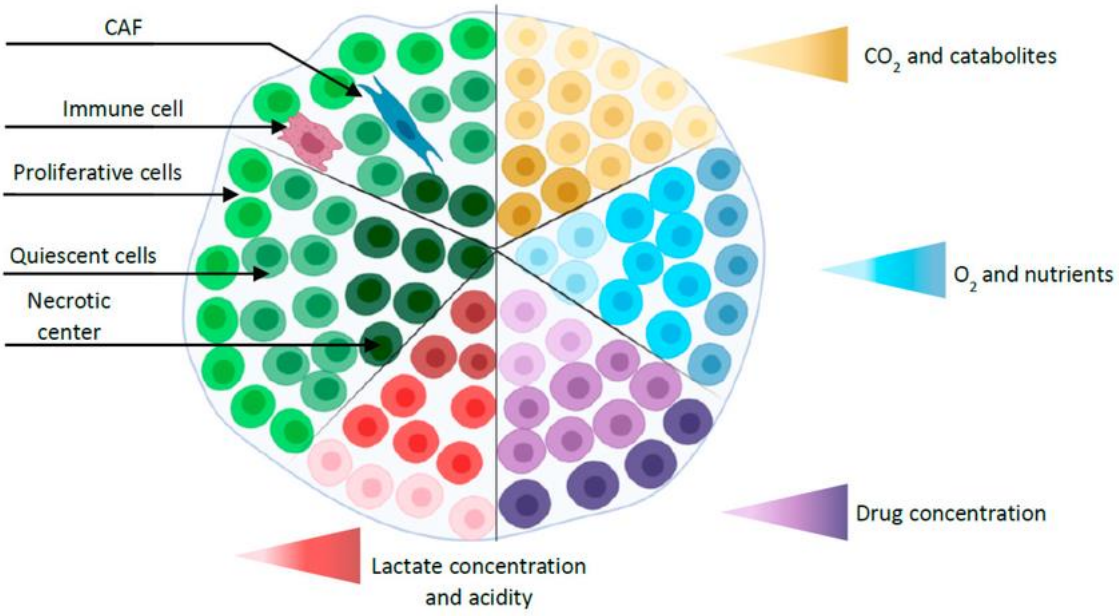

Figure 1.: Schematic representation of layers and gradients in a co-culture spheroid (Alzeeb et al., 2020).

2.3 2D vs 3D cell culture

Cultivation of cell lines in a 2D environment has been used for over a century and still works on the same principle: cells are grown in a culture bottle or petri dish where they attach to a surface. However, these conditions do not mimic the natural environment of tissues. They create unrepresentative conditions that do not reflect the fundamental intercellular interactions crucial for cell growth, cell viability, and protein and gene expression.

Morphological changes may occur when cultured in 2D. Cells lose their polarity due to disrupted interactions with the external environment. Moreover, in the culture bottle, cells have unrestricted access to oxygen and nutrients from the medium, which does not correspond to the physiological variability present in tumour tissues (Kapałczyńska et al., 2016).

Culturing cells in a 2D environment offers many advantages, making this method popular in clinical development and research laboratories. One of the main advantages is the simplicity of the process, as it does not require complex and expensive equipment. Working with 2D cultures also ensures high reproducibility due to consistent culture conditions, facilitating fast and easy experiment reproduction.

In addition, several well-standardized protocols for culturing cells in a 2D environment simplify analysis. Thus, most analytical methods are readily applicable to 2D cultures. Other advantages are simple viability detection and the possibility of genetic modification.

One of the primary benefits of 3D cell lines, specifically spheroids, is their ability to more accurately mimic the natural arrangement of cells by forming a three-dimensional structure. This structure better mimics physiological conditions typical for tumor tissues, such as the oxygen gradient and nutrient distribution. Cells within the spheroids form intercellular interactions similar to those in a living organism, allowing more detailed study of cell signaling and gene expression with greater biological relevance. In addition, spheroids are highly scalable, suitable for high-throughput screening, and are finding applications in personalized medicine (Yun et al., 2024).

Using 3D cell cultures also brings challenges, such as technically demanding preparation requiring specific and more costly resources. Visualization can also pose problems, as the radiation source penetrates the spheroid layers less effectively. Many protocols established for 2D cell lines cannot be used for 3D cultures and must be optimized. Furthermore, sample analysis is generally more complex, as there is a lack of commercially available products optimized for 3D cultures, which means spheroids are not commonly used in routine clinical laboratories (Cianciosi et al., 2021).

In summary, each cell culture method brings several specific advantages and disadvantages that affect their use in research. The choice of the culture method should consider practical and financial aspects and the biological relevance of the results. The basic differences between the two types of cell cultures are described in Figure 2.

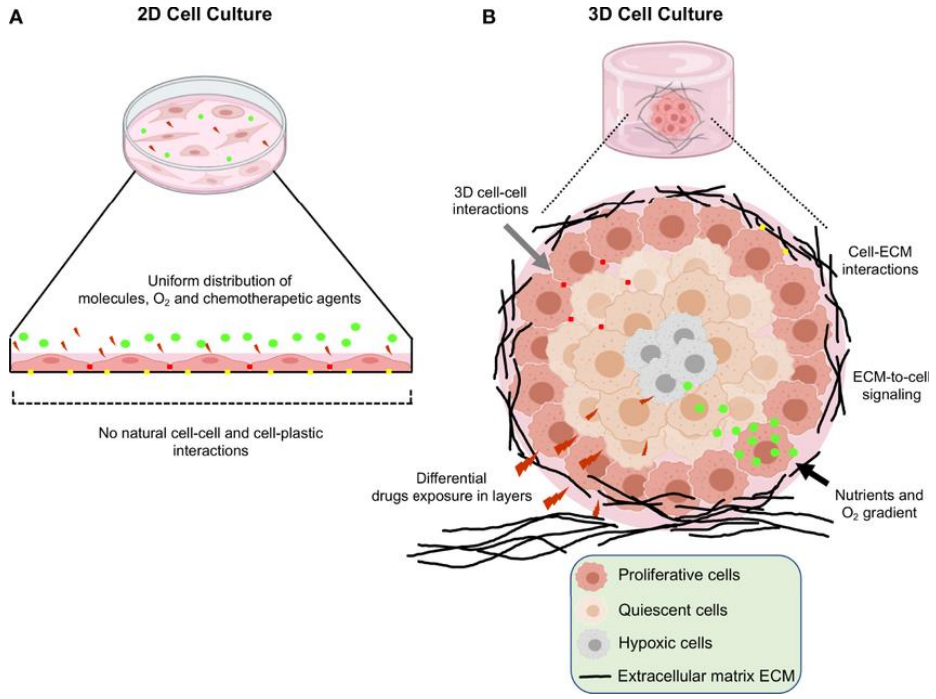

Figure 2: Illustration of the differences between 2D and 3D cell cultures. (**A**) In 2D cell culture, cells grow in a monolayer on the bottom of culture bottoms. They have unlimited access to nutrients, oxygen and drugs. Intercellular interactions are limited. (**B**) 3D cell culture, more cell-to-cell and ECM, and limited access to nutrients and oxygen better mimic the tumor microenvironment (Salinas-Vera et al., 2022).

2.4 Methods of spheroid preparation

2.4.1 Hydrogels

One of the spheroid culture systems is hydrogels that mimic the extracellular matrix (ECM) of proteins, glycosaminoglycans, and glycoproteins. The ECM is crucial for cell adhesion, tissue mechanical stability, and cell growth and proliferation regulation. Therefore, the hydrogel environment provides cells with biophysical and biochemical stimuli that are also present under in vivo conditions.

Commonly used protein-based hydrogels include Matrigel. This is the commercial name for the solubilized basement membrane matrix secreted by Engelbreth-Holm-Swarm mouse sarcoma cells (Hughes et al., 2010). Matrigel polymerizes at 37°C, and thanks to the presence of growth factors, e.g. stem cells can grow on it. Wang et al., 2020 have shown that Matrigel promotes the survival of neural stem cells *in vitro* and *in vivo*. Rats with spinal cord damage who received the transplant showed improved behavioral recovery and increased expression of astrocytic and neuronal markers compared to controls.

Another type of hydrogel is polysaccharides, which include, for example, hydrogels made of hyaluronic acid or agarose. These hydrogels are useful because, unlike Matrigel, they provide stable conditions for spheroid growth. Their degradation is not dependent on proteolytic enzymes secreted by the cells, as is the case with hydrogels made from collagen or Matrigel (Y. Li & Kumacheva, 2018).

2.4.2 Agarose overlay method

Agarose is a natural polysaccharide polymer and, together with agropectin, is part of the agar obtained from red algae. It consists of alternating galactose and 3,6-anhydrogalactose subunits. Due to its excellent biocompatibility, affordability, and thermoreversible behaviour, it has found applications not only for spheroid formation but also for, for example, DNA separation by gel electrophoresis.

384-well plates can be coated with agarose, and spheroids subsequently cultured in them, allowing high throughput screening of, e.g., drug efficacy, evaluation of spheroid viability by confocal microscopy, and various cytotoxicity essays. (Das et al., 2016).

In this thesis, agarose-coated plates were used for spheroid formation because the agarose-overlay method allows rapid cell aggregation and quantitative and qualitative analysis of individual spheroids. Cultivation of spheroids on both agarose and hydrogels generally provides the formation of spheroids of homogeneous size and allows for consistent evaluation of the experiments performed (Gong et al., 2015).

2.4.3 Hanging drop

The hanging drop method belongs to the scaffold-free techniques, i.e., techniques for culturing cells in a 3D environment without using support materials. The basic principle of this method is to create tiny drops, usually 20 μL of cell suspension, which hang on the inside of a cultivation surface (e.g. a Petri dish). After pipetting the suspension, the cap is turned upside down to form a hanging droplet held by surface tension. The effect of gravity concentrates the cells at the bottom edge of the drop, which promotes contact between them and facilitates the formation of spheroids.

The hanging drop method is characterized by its simplicity - it does not require complex or expensive laboratory equipment and finds applications in basic research. Another advantage is the possibility of co-culturing cells of different types, allowing the modeling of complex cellular environments or observing intercellular interactions.

However, the hanging drop method also brings with it several disadvantages, significantly when changing the medium or adding different substances, e.g. when testing drugs. The limited drop volume also reduces the efficiency and accuracy of the work, making the hanging drop method unsuitable for applications requiring high throughput screening (Rasouli et al., 2024).

The possibilities of using this method in high throughput screening were described by (Tung et al., 2011), who presented a 384-well plate made of polystyrene. Each well of this plate contains an access hole that allows easy medium exchange. The edges of the plate are equipped with small water reservoirs that prevent evaporation of the medium and stabilize its osmolality.

2.4.4 Microfluidic device

Microfluidic devices are another widely used method for producing spheroids. In these devices, microscopic channels carefully control the environment where cells aggregate to form spheroids. These devices allow the monitoring of conditions such as oxygen distribution, nutrient supply uniformity, and optimum pH, factors that are essential for the successful formation and maintenance of healthy spheroids (Tevlek et al., 2023).

Microfluidic technologies can be divided into two main categories: continuous flow and digital microfluidics. Continuous flow means fluid flows through the microchannels continuously and without interruption. It is used, for example, to monitor processes that require a continuous supply of oxygen and nutrients. Digital microfluidics, on the other hand, allows precise manipulation of individual fluid droplets by electrical or mechanical forces. This approach has applications where small and separated fluid volumes must be handled, for example, when testing different drugs (Yu et al., 2010).

Single-phase microfluidics, which includes perfusion microfluidics, enables spheroid growth using a perfusion system that simulates natural blood flow conditions. In contrast to classical spheroid culture, this approach allows long-term growth of 3D cultures without a significant decrease in cell viability (Hu & Li, 2007).

As mentioned, digital microfluidics combines microfluidic devices and electrical forces to manipulate individual fluid droplets. Two approaches are used to culture cells: a closed format, where droplets of cell suspension are enclosed between two plates, and an open format, where droplets are placed on a surface. The bottom plate contains the electrodes, while the top plate is usually transparent in the case of the closed format, allowing for optical sensing. All manipulation of the droplets is performed by electrostatic force, where the electrical potential of the electrodes is adjusted to enable the movement of the droplets. Classical digital microfluidics was designed to work on 2D platforms, but to move to 3D environments, droplets are immersed in oil between electrodes, allowing droplet manipulation in both horizontal and vertical directions (Cho et al., 2003).

The above methods are illustrated in Figure 3.

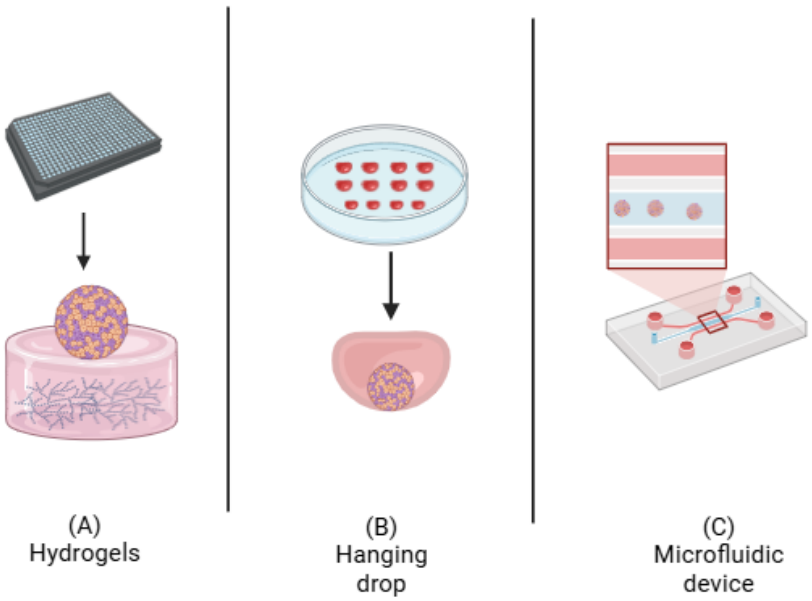

Figure 3: Graphically characterized spheroid culture system methods. (**A**): hydrogels, (**B**) hanging drop, (**C**) microfluidic device. Created with BioRender.

2.5 Drug testing on spheroids

Drug testing for cancer is essential to research to create more effective therapies. This process has multiple steps, from laboratory testing to clinical trials. Research commonly starts with *in vitro* models, like two-dimensional cell cultures. However, 3D models, such as spheroids or organoids, are increasingly used since they more closely mimic the natural tumor environment.

Another method that can be used to test therapeutic drugs is so-called "animal models," such as the zebrafish, which allow *in vivo* visualization of tumor cells as they migrate, proliferate, or even respond to treatment (Astell & Sieger, 2020). Humanized mouse models are increasingly being used, but both variants have limitations as they are not fully capable of providing an environment corresponding to human biology (Malaney et al., 2014).

Anticancer drug development is increasingly focused on the ability to target specific mutations and signaling pathways that are key to cancer cell growth and survival or characteristic of certain types of cancer and other diseases. Modern approaches include the combination of chemotherapy with immunotherapy, using graphene-based conjugates and nanotechnology to enable precise drug delivery directly to tumor tissue (Chatzinikolaidou, 2016).

The current research aims to develop spheroid models for anticancer drug testing that could increase the accuracy of drug effect prediction, reduce the need for animal testing, and reduce the overall cost of new drug development. To accelerate the development of these models, it is essential to standardise the numbers of cells from which spheroids are formed and to provide optimal culture conditions that are suitable not only for high throughput screening but also for ensuring a constant supply of nutrients, similar to that provided by microfluidic devices. Indeed, different methods of cultivating spheroids may lead to different responses to drugs (Hickman et al., 2014).

To use spheroids more effectively as models for testing anticancer drugs, it is important to understand how these drugs are distributed and how they penetrate across spheroids. This could be aided by a method that assesses the distribution of therapeutics in spheroids using a combination of sequencing trypsinization and nanoflow liquid chromatography-tandem mass spectrometry (nLC-MS/MS) (Liu & Hummon, 2015). This

method quantitatively measured irinotecan and its active metabolite SN-38 in different spheroid regions formed by HCT116 colorectal cancer cells. Specifically, the drug permeability was time-dependent, and SN-38 was more abundant in the spheroid's outer edges and middle layer. Therefore, this and other similar methods can be used to identify drug distribution characteristics and can also aid in the process of the overall evaluation of drug effects.

This thesis was focused on the study of the effect of selected drugs on spheroids, namely 5-fluorouracil, irinotecan, and cisplatin, that Vrablíková, 2022 should show a synergistic effect in spheroids.

5-fluorouracil is a chemotherapeutic drug, classified as a synthetic analogue of pyrimidine, which can inhibit enzymes involved in DNA and RNA synthesis. Similar in structure to uracil, it is metabolized upon entry into cells to an active form that inhibits thymidylate synthase, thereby depleting thymidine. 5-fluorouracil acts on proliferating tumor cells exposed to DNA damage and undergo apoptosis due to its action. However, chemotherapy using 5-fluorouracil also damages non-tumor cells such as bone marrow and digestive tract cells (N. Zhang et al., 2008).

Cisplatin is a metal complex compound that is classified as a platinum drug. Upon entering the nucleus, it forms a covalent bond with DNA. This formed adduct prevents DNA replication and transcription, leading to cell damage and subsequent apoptosis. Additionally, cisplatin is also known to cause nephrotoxicity, leading to acute kidney failure. This toxicity limits its widespread use and requires careful monitoring of patients (Miller et al., 2010).

The last of the drugs used in this thesis is irinotecan, an inhibitor of topoisomerase I, an enzyme involved in DNA replication, which takes care of the release of tension arising from DNA unraveling. When irinotecan enters cells, it is converted into its active form, SN-38, blocking topoisomerase I, which leads to the formation of breaks in the DNA molecule. By this mechanism, it has a significant effect on cancer cells that have defects in DNA repair.

2.6 Spheroids as a physiologically-relevant tumor model

Since spheroids can replicate the human body's three-dimensional environment and physiological circumstances, they offer a wide range of uses in biomedical research. As a result, they serve as flexible models with a wide range of applications in several fields, which are discussed in this chapter.

Spheroids increasingly find applications in tissue engineering, a technological process that creates, repairs, and improves biological tissues or organs. Many advances have been made in recent years; for example K. Zhang et al., 2015 have designed a non-adhesive scaffold that stimulates in situ spheroids assembly from mesenchymal stem cells (MSC). After the implantation of spheroids into damaged articular cartilage of rabbits, chondrogenesis and overall cartilage regeneration were promoted.

Spheroids cultured without scaffolds could be even better used in regenerative medicine, which eliminates the subsequent biocompatibility problems encountered during implantation. For example**,** MSC-derived spheroids were prepared from human bone marrow by rotational culture without using scaffolds. Then, these spheroids were implanted into skull defects in rats, promoting bone regeneration. (Suenaga et al., 2015).

Spheroids are also used experimentally in cell therapy, as they are functionally more advanced than single-cell suspension. In studies, cells injected as spheroids have been shown to achieve more prolonged survival *in vivo* than if injected as a single-cell suspension (Suryaprakash et al., 2019). Furthermore, salivary gland stem cells (SGSCs) injected into irradiated salivary glands showed better therapeutic effects than delivery as single cells (Ko et al., 2021). This approach suggests that 3D cultures may be more effective and may provide greater cell therapy efficacy.

The use of spheroids in personalized medicine is also expected to increase. Although spheroid models derived from cell lines, such as the HCT116 line used in this thesis, appear to be sufficient for modeling the tumor microenvironment, greater accuracy is afforded by cells from primary tumor tissue (Carter et al., 2021). Specific spheroid models derived directly from patients can accurately mimic the transcriptional profile of the tumor and are also suitable for high-throughput screening (Sato et al., 2011).

The same techniques can also be used for culturing patient spheroids and spheroids from cell lines. In addition, they are also able to faithfully mimic intercellular integration,

gene expression, and the hypoxic gradient (Zhu et al., 2022). However, their main drawback is their limited ability to model the TME due to the absence of a well-defined ECM, which prevents cells from self-organizing into 3D structures that mimic in vivo tumors. As a result, patient organoids are still more widely used than patient spheroids, even though spheroids are less expensive and easier to handle (Bregenzer et al., 2019).

Spheroids also appear to be a relevant model for studying their use in immunotherapy, owing to their ability to simulate the tumor microenvironment. Some studies suggest that spheroids appropriately represent how *in vivo* tumors "escape" immunotherapies. For example, it was observed that spheroids were able to reduce the expression of human leukocyte antigen (HLA) derived from T-lymphocytes, which, in contrast, the same cell type cultured in monolayer was unable to do (Busse et al., 2013).

Furthermore, it was found that HT29 colorectal cancer spheroids showed better natural killer (NK) cell infiltration compared to T cell infiltration efficiency. NK cells showed efficient infiltration despite the dense barriers in the tumor spheroids, whereas antibodies could not penetrate the spheroids (Courau et al., 2019). Tumors often have hypoxic areas that negatively affect the efficacy of immunotherapy. Spheroids can model hypoxic areas and study how different immunotherapeutic strategies, including combination with other drugs, can overcome this problem (Ai et al., 2015).

2.7 Future trends in 3D culture development

The development of spheroids in the context of their use in medical research continues to move forward to introducing spheroids into clinical laboratories. Their use is possible, for example, in personalized medicine, specifically in testing drugs on spheroids to optimize the treatment of specific patients. In this case, however, improving and standardizing methods for forming homogeneous spheroids and measuring their viability or proliferation is necessary.

As the first one, the so-called bioprinting of spheroids could revolutionize research. As the name suggests, this technology uses 3D bioprinting to create highly precise three-dimensional cell aggregates with predefined structures.

However, current approaches to spheroid formation using scaffolds often expose living cells to shear stress, heat, or toxic chemicals, which can be lethal to cells (Jungreuthmayer et al., 2009). With a few exceptions, another obstacle is the lack of a biomaterial to support different cell types. If such a biomaterial already exists, it is patented by a specific company, which limits access to research and increases financial costs.

Numerous bioprinting techniques have developed due to modern technologies, each suited to the unique requirements and objectives of a particular research. For example, the extrusion-based bioprinting technique works effectively for creating spheroids of various sizes. On the other hand, the Kenzan approach offers excellent resolution and accuracy, is highly scalable, and enables the construction of larger and more complex structures. Furthermore, the droplet-based approach provides quick and easy bioprinting of spheroids, which is beneficial for applications that do not require the creation of intricate structures (Banerjee et al., 2022).

One method that will become increasingly common in 3D lines in the future is an organ-on-chip (OOC). Although 3D cultures are a better option than 2D cultures, they cannot mimic more complex physiological functions such as blood circulation and interstitial flow at the organ level. The OOC method has this unique feature (Cao et al., 2023).

However, for complex pharmacokinetic and pharmacodynamic studies, multiple such systems are needed to simulate the interaction of organs through the vasculature. (Novak et al., 2020), have, therefore, developed a device called the "interrogator" that automates

culture, perfusion, media exchange, channel interconnection, sampling, and in situ microscopy of up to ten organ-on-chips in an incubator. The interrogator kept eight vascularized organ models (e.g., intestine, liver, kidney, brain) functional for three weeks, simulating their connection via a common blood substitute. The technology allowed quantitative monitoring of the distribution of substances between the models and repeated sampling of vascular and interstitial compartments without disrupting the system, opening up new possibilities for drug testing and modeling physiological processes at the human body level.

3 Materials and methods

3.1 List of biological material

All cell lines were obtained from the Biobank of the Institute of Molecular and Translational Medicine, Faculty of Medicine and Dentistry, Palacky University Olomouc. T-cell lymphocytes were isolated from discarded blood samples of normal blood donors from the Transfusion Department of the University Hospital Olomouc. No ethical approval was required since these samples are typically discarded after transfusions, using only erythrocytes, plasma, and platelets.

- HCT116 parental
- HCT116 parental-GFP
- HCT116 p53 -/-
- HCT116 p53 +/-
- HCT116 R248 w/-
- HCT116 KRAS +/-
- HCT116 G13D/-
- CCD18-Co
- Lymphocytes

3.2. List of chemicals, reagents, solutions

- Dulbecco's Modified Eagle Medium (DMEM) (Lonza, Cat. # BE12-719F)
- Minimum Essential Medium Eagle (EMEM) (Gibco, Cat. # 16209961)
- McCoy's 5A media with L-glutamine (Lonza, Cat. # 12-688F)
- 10% fetal bovine serum (FBS) (Gibco, Cat. # 26140079)
- 1% penicillin/streptomycin (Capricorn, Cat. # PS-B)
- Trypan blue (Sigma Aldrich, Cat. # T6146)
- Low-melting agarose (Sigma-Aldrich, Cat. # A9414)
- Copper diethyldithiocarbamate (CuET) (Sigma-Aldrich, Cat. # D3506)
- Interleukin-2 (IL-2) (Peprotech, Cat. # 200-02-50UG)
- Ethylenediaminetetraacetic acid (EDTA) (Sigma Aldrich, Cat. # E26290)
- Lymphopure™ (BioLegend, Cat. # 426202)
- Propidium iodide (Sigma Aldrich, Cat. # P4864)
- CellTiter-Glo® Cell Viability Assay (Promega, Cat. # G7570)
- 5-fluorouracil (Ebewe; obtained from University Hospital in Olomouc)
- Cisplatin (Ebewe; obtained from University Hospital in Olomouc)
- Irinotecan (Ebewe; obtained from University Hospital in Olomouc)
- PierceTM BCA Protein Assay Kit (ThermoFisher, Cat # 23225)
- 10% separating gel for SDS PAGE (Tab. 3)
- 4% stacking gel for SDS PAGE (Tab. 4)
- 10x Lammli sample buffet (Tab.5)
- Ponceau S (Sigma Aldrich, Cat. # 141194)
- 5% bovine serum albumin (BSA) (Sigma Aldrich, Cat. # A9418)
- Polyclonal primary antibodies
    - Acetyl-α-Tubulin Lys40 #3971 (Cell Signaling Technology)
- Monoclonal primary antibodies
    - p21 Waf1/Cip1 (12D1) Rabbit mAb #2947 (Cell Signaling Technology)
- Secondary antibodies
    - Goat anti-mouse IgG (H+L) Superclonal™ Secondary Antibody, Alexa Fluor™ 488 (Invitrogen)
    - Goat anti-Rabbit IgG (H+L) Cross-Adsorbed Secondary Antibody, Alexa Fluor™ 488 (Invitrogen)
- Spectra™ Multicolor Broad Range Protein Ladder (ThermoFisher, Cat. # 26634)
- Tris-buffered saline with Tween 20 (TBS-T) (Tab. 6)
- 10x phosphate buffer (PBS) (Tab. 1)
- TrypLe enzyme (Thermo Fisher, Cat. # 12604013)
- RIPA Lysis and Extraction Buffer (Thermo Fisher, Cat. # 89901)
- Halt™ Protease and Phosphatase Inhibitor Cocktail (100X) (ThermoFisher, Cat. # 78440)

3.3 List of equipment

- Thermo Scientific Cytomat 10C Automated Incubator
- Laminar flow box MSC-Advantage™
- Hettich® ROTINA 420/420R centrifuge (Hettich GmbH & Co. KG.)
- Eppendorf® Centrifuge 5810 G (Eppendorf AG)
- Tissue Culture Flasks 25 - 300 cm2 (TPP)
- Eppendorf pipettes (0.5–1000 µl) (Eppendorf AG)
- Vi-CELL XR Cell Viability Analyzer (Beckman Coulter, Inc.)
- Microwave oven (Hitachi)
- -80°C and -20°C freezer (New Brunswick Scientific)
- 96 well plate (TPP)
- 384 well plate (BioRad)
- MultiDrop dispenser (Thermo Fisher)
- Axio Observer D1 Fluorescent microscope (Carl Zeiss)
- CERTUS FLEX low-volume liquid dispensing (Nnano)
- EnVision plate reader (PerkinElmer)
- Branson 450 Digital Sonifier (Branson)
- Tecan Infinite M1000 Pro (Tecan Group Ltd)
- Electrophoresis chamber (Bio-Rad)
- Trans-Blot Turbo (Bio-Rad)
- Thermoblock (Eppendorf)
- ChemiDoc MP system (BioRad)

3.4 Cell culture and growth conditions

In this thesis, the CCD18-Co cell line, which is normal colon fibroblasts, and the HCT116 colorectal cancer cell line, along with its mutant forms listed in Materials and Methods were used. Fibroblasts were grown in EMEM supplemented with 10% FBS and 1% antibiotic (penicillin/streptomycin). Colorectal cancer cells were grown in McCoy's medium supplemented with 10% FBS and 1% antibiotic (penicillin/streptomycin).

Both cell lines were maintained in an incubator at 5% CO_2 and 37°C. Cells were passaged every 3–4 days upon reaching 80-90 % confluency. Before each passage, the media, 1x PBS (stock solution described in Tab.1), and TrypLe enzyme were pre-warmed in a water bath at 37°C. This type of environment mimics the physiological conditions of the human body. After pouring the original medium into a pre-prepared waste bottle disinfectant, 2 x 5 mL of PBS was added to remove the residual original culture medium and maintain osmolarity. As part of the dissociation of cells from the surface of the culture flask, TrypLe enzyme was added, typically 0.5 mL per 10 cm^2. The culture flask was placed in an incubator at 37°C for 3 minutes to ensure proper cell detachment. The enzymatic reaction was subsequently stopped by adding 5 mL of complete medium. This suspension was then transferred to a 50 mL Falcon tube, and the cells were centrifuged for 5 minutes at 45 x g (G-force). The resulting pellet was resuspended in 5 mL of culture medium, and cell viability was determined using the Vi-CELL XR Cell Viability Analyzer, which employs trypan blue for viability assessment. Cell lines with viability greater than 90 % were always used for experiments. All cell lines used in this thesis were regularly tested for mycoplasma.

Tab.1: Composition of 10X PBS Solution (1 Liter)

Component	Amount Required
Sodium chloride (NaCl)	80 g
Potassium chloride (KCl)	2 g
Disodium phosphate (Na_2HPO_4) (anhydrous)	14.4 g
Potassium dihydrogen phosphate (KH_2PO_4)	2.4 g
Distilled water (to final volume)	Up to 1 liter
pH Adjustment (HCl or NaOH)	As needed to pH 7.4

3.5 Spheroid Formation Using Agarose-Coated Plates

Spheroids were generated using the method previously established in the lab (Das et al., 2015). Agarose (0.75 g w/v) was solubilized in DMEM media using microwave heating and sterilization by autoclaving. The resulting agarose solution was subsequently used to coat 96- and 384-well plates, dispensing 50 µL and 15 µL of agarose per well, respectively, using a MultiDrop Semiautomated dispenser. The coated plates were then stored at 4°C and used within one month from preparation.

Before cell seeding, the plates were equilibrated to room temperature (RT). For all experiments involving primary lymphocytes, cancer cells were seeded at a density of 5,000 cells/well. Cells were seeded at 7:3 (HCT116: CCD18-Co) and 3:7 (HCT116:CCD18-Co) ratios to assess drug synergy in co-culture, with a total cell density of 5,000 cells/well. Following inoculation, the plates were allowed to rest for 30 minutes, after which centrifugation was performed at 4 x g for 20 minutes. Over a period of three days, the cells aggregated into spheroids, which were subsequently utilized for experiments.

3.6 Cultivation and stimulation of lymphocytes for spheroid treatment

In this thesis, spheroids from different mutant lines of colorectal cancer (listed in section 3.2.) were used as a model to test their interaction with three types of lymphocytes: unstimulated control lymphocytes, lymphocytes stimulated with copper diethyldithiocarbamate (CuET), and lymphocytes stimulated with interleukin 2 (IL-2). It has been proven that lymphocytes stimulated with 1 nM CuET exhibited increased cytotoxicity against tumor cells; however, this testing was conducted on classical two-dimensional culture systems (Pokorná, 2022) . Moreover, it has been shown that IL-2 can significantly boost the ability of lymphocytes to kill tumor cells, which are then eliminated (Oshimi et al., 1986).

Lymphocytes were isolated from the blood of normal human donors by Prof. Juan De Sanctis and his group. Briefly, the Ficoll-Hypaque method was used to isolate lymphocytes from the blood. The patient's blood obtained from the Transfusion Department of the University Hospital in Olomouc was transferred to a tube containing the chelating agent EDTA and then diluted with phosphate buffer. For every milliliter of blood, 0.5 mL of Lymphopure™ was added, ensuring that the Lymphopure™ solution remained at the bottom of the tube without mixing with the blood. The conical tube was centrifuged at RT at 800 x g for 20 minutes. After centrifugation, four phases can be observed in the tube: at the bottom, is a phase of erythrocytes and granulocytes; above it is the PBS phase, followed by the phase of isolated mononuclear cells containing the desired lymphocytes. The final top phase is blood plasma.

The isolated mononuclear cells were subsequently washed and transferred to a culture flask containing medium. Typically, the cell population consists of approximately 70-75 % T lymphocytes, 10-15 % B cells, and 5-12 % NK cells. After adhering to the surface of the flask, the cells were stimulated with 1 nM CuET and 10 ng/ml IL-2 for 12 hours.

Three-day-old spheroid monocultures of seven different colorectal cancer cell lines, consisting of 5,000 cells per well, were subsequently treated with unstimulated lymphocytes, CuET-stimulated lymphocytes, and IL-2-stimulated lymphocytes at three different concentrations: 25,000 lymphocytes per spheroid, 50,000 lymphocytes per spheroid, and 100,000 lymphocytes per spheroid. The treatment lasted for 72 hours and was performed in three independent experiments. The experiment was performed in 3 biological replicates.

3.7 Fluorescence microscopy

Fluorescence microscopy is a highly sensitive and specific imaging technique that allows the visualization of cellular and tissue structures using fluorescent dyes. The process begins with an intense light source, such as a mercury lamp, which illuminates the sample. This light then passes through an excitation filter with a specific wavelength to excite the fluorophores. Subsequently, the emitted light, which has a longer wavelength than the excitation light, is filtered through an emission filter and captured by a camera.

After three days of treatment with lymphocytes, the spheroids were stained using 1 mg/mL propidium iodide (PI). This hydrophilic fluorescent dye binds to the DNA of dead or damaged cells, as their cell membrane integrity has been compromised. After a 10-minute incubation with PI, the intensity of the fluorescent signal was analyzed using an Axio Observer D1 Fluorescent microscope (Carl Zeiss). Propidium iodide emits red light at a maximum wavelength of 636 nm. The Zeiss Zen Blue software was used for image analysis, facilitating both image processing and quantitative assessment of fluorescence intensity.

3.8 Luminescent cell viability assay

For the determination of spheroid viability, the CellTiter-Glo Assay from Promega was utilized. This luminescence method is based on measuring the level of adenosine triphosphate (ATP), which reflects the viability of cells (Fig.4). The assay is highly sensitive, rapid, and suitable for assessing spheroid viability. Other methods, such as the MTT or MTS assays, are not as appropriate, particularly due to the complex structure of spheroids, which complicates substrate accessibility.

Prior to the assay, plates containing the spheroids were equilibrated at RT for approximately 30 minutes. Subsequently, 25 µL of the medium was removed from each well, and 25 µL of reagent was added using the Certus Flex liquid dispenser. The plates were then shaken on an orbital shaker to facilitate spheroid lysis and enhance the release of the targeted ATP. After a 25-minute incubation period with the reagent, the intensity of luminescence was measured using the EnVision plate reader. The data was analyzed using Microsoft Excel.

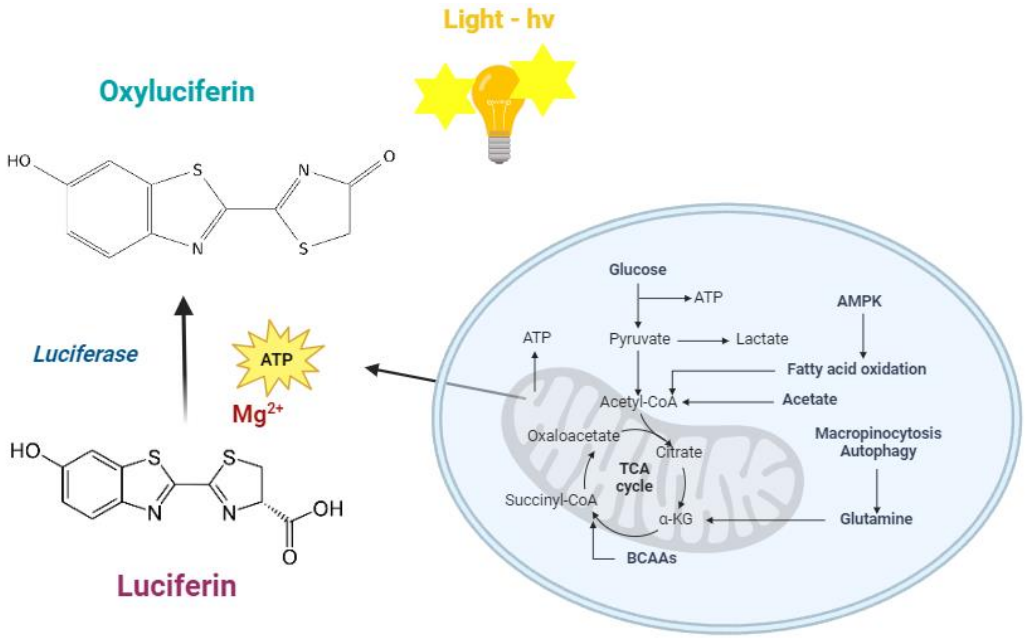

Figure 4: Principle of the luminescence method for the determination of spheroid viability by the ATP-dependent luciferase reaction. Created with Biorender.

3.9 Synergy studies

To analyze the effect of drug combinations with synergistic effect at the molecular level, 4 groups of spheroids (5000 cells/spheroid) were created - spheroids formed only by HCT116-GFP cells, - spheroids formed only by CCD18-Co cells, spheroids in a 7:3 ratio (HCT116:CCD18-Co) and spheroids in a 3:7 ratio (HCT116:CCD18-Co). These proportional combinations of spheroids were used because they better mimic the physiological model of the tumor. Based on the diploma thesis Vrablíková, 2022, ratio combinations of the drugs 5-fluorouracil, cisplatin, and irinotecan show a synergistic effect. This effect had to be verified at the molecular level. Spheroids were then treated with the following drug combinations: 1:1 5-fluorouracil: cisplatin, 1:2 5-fluorouracil: cisplatin, and 4:1 irinotecan: cisplatin (Tab. 2) and incubated with the drugs for 7 days. For one test sample, 96 spheroids were used. The experiment was performed in 3 biological replicates.

Tab. 2: Drug combinations used for different spheroid types.

HCT116-GFP	7:3 spheroids	3:7 spheroids	CCD18-Co
1:1	1:2	1:1	1:1
1:2	4:1	4:1	1:2
4:1	X	X	4:1

3.10 Protein isolation

After seven days of treating the spheroids with various combinations of drugs, the spheroids were gently pipetted out of the well and transferred to a 50 mL tube. Spheroids were then allowed to sediment, and after sedimentation, the excess medium was replaced, and 1 mL of TrypLe was added to the tube. Spheroids were incubated with TrypLe in an incubator at 37°C for 5 minutes. The spheroids were disintegrated into single-cell suspension by gently pipetting them several times. The spheroids were then separated from TrypLE and the remaining medium by centrifugation at 45 x g for 3 minutes at RT. The pellet was resuspended in 1 mL PBS and transferred to an Eppendorf tube.

The samples were subsequently separated again by centrifugation from PBS at 45 x g for 3 minutes at RT, and the resulting pellet was resuspended in 50 µl of RIPA buffer enriched with phosphatase and protease inhibitors at a 50:1 ratio. These prepared samples were subjected to sonication for cell lysis using a Branson 450 Digital Sonifier with settings at 25% amplitude 10s pulse on, and 10s pulse off. This was followed by centrifugation at 50 x g for 30 minutes at 4°C. The resulting supernatant was transferred to an Eppendorf tube and stored at -80°C.

3.11 BCA assay

For the detection and quantification of total proteins in the samples, a BCA (bicinchoninic acid) assay was used. This method is based on the reaction of BCA with copper in an alkaline environment, where proteins reduce the copper ions, forming a purple-colored complex. The BCA reagent solution was prepared by mixing BCA solution and 4% copper sulfate ($CuSO_4$) solution in a 50:1 ratio. Subsequently, 100 µl of BCA reagent and 10 µl of Pierce™ Bovine Serum Albumin Standard were added to a microtiter plate. The samples were added to the BCA reagent at 2 µl each. The mixtures were then incubated at 37°C for 30 minutes. Absorbance was measured spectrophotometrically at 562 nm by Tecan Infinite M1000 Pro, and protein concentrations were calculated based on a calibration curve.

3.12 Western blot

Protein electrophoresis on a polyacrylamide gel in the presence of sodium dodecyl sulfate (SDS PAGE) was used to separate proteins according to their molecular weight. Separating gel was prepared first (Tab. 3), followed by the stacking gel (Tab. 4). Proteins were mixed with sample buffer (Tab. 5) so that the final amount of protein was applied to the well with the sample buffer was 20 ug/well. The electrophoretic chamber was filled with 1x Tris-glycine-SDS running buffer, allowing electrical current transfer. Electrophoresis was carried out for 90 min at a current of 120 V.

Subsequently, protein transfer to the nitrocellulose membrane was performed using Trans-Blot Turbo and the success of the transfer was verified using Ponceau S dye. Membrane blocking was performed in 5% BSA for 1 hour at RT to avoid non-specific binding during antibody detection. Polyclonal antibody Acetyl-α-Tubulin Lys40 #3971 (Cell Signaling Technology) and monoclonal antibody p21 Waf1/Cip1 (12D1) Rabbit mAb #2947 (Cell Signaling Technology) were used as primary antibodies. All primary antibodies were diluted 1:1000 and incubated with the membrane overnight at 4°C with gentle shaking. Subsequently, the membrane was washed 3 times in 1x TBS-T (Tab.6) for 10 min. Goat anti-mouse IgG (H+L) Superclonal™ Secondary Antibody, Alexa Fluor™ 488 (Invitrogen) and Goat anti-Rabbit IgG (H+L) Cross-Adsorbed Secondary Antibody, Alexa Fluor™ 488 (Invitrogen) were used as secondary antibodies. Both secondary antibodies were diluted 1:2000 and incubated with the membrane for 1 hour at 4°C with gentle shaking. Subsequently, the membrane was washed 3 times in TBS-T for 10 minutes. Visualization was performed using the ChemiDoc MP system (BioRad). ImageJ software was used to determine the band density.

Tab. 3: Composition of 10% separating gel (10 mL).

30% Acrylamide/Bis-acrylamide	3.3 mL
1.5 M Tris-HCl (pH 8.8)	2.5 mL
10% SDS	100 µL
10% APS (Ammonium Persulfate)	100 µL
TEMED	10 µL
Distilled Water	4.0 mL

Tab. 4: Composition of 4% stacking gel (10 mL).

30% Acrylamide/Bis-acrylamide	0.67 mL
0.5 M Tris-HCl (pH 6.8)	1.25 mL
10% SDS	50 µL
10% APS (Ammonium Persulfate)	50 µL
TEMED	5 µL
Distilled Water	3.0 mL

Tab. 5: Composition of 10x sample (Laemmli) buffer

1 M Tris-HCl (pH 6.8)	1.5 mL
20% SDS	1 mL
Glycerol (80%)	2 mL
β-mercaptoethanol (BME)	0.5 mL
Bromophenol Blue (0.04%)	10 µL

Tab.6: Composition of 10x TBS-T

Tris (Tris base)	3.03 g
Sodium chloride (NaCl)	8.0 g
Tween 20	0.1 mL
Distilled water	Up to 1 liter

4 Results

4.1 HCT116 parental

4.1.1 Quantitative Assessment of Cellular Energy

The evaluated luminescence data (Fig. 5) for spheroids from the HCT116 line show that in the first group when spheroids were treated with control lymphocytes, reported an increase in luminescence with increasing lymphocyte concentration. The largest change is observed in the 100,000 lymphocytes/spheroid.

In spheroids treated with 1 nM CuET, luminescence is most intense at 100,000 lymphocytes/spheroid, indicating that the higher concentration has a more significant effect. At concentrations of 25,000 and 50,000, the effect is lower, but the values are comparable to those of the first control group.

In the third group, where lymphocytes were treated with IL-2, luminescence increased at 25,000 lymphocytes/spheroid, which may demonstrate their effectiveness at low concentrations. The other two groups show decreased luminescence, which may indicate cytotoxicity at higher lymphocyte concentrations.

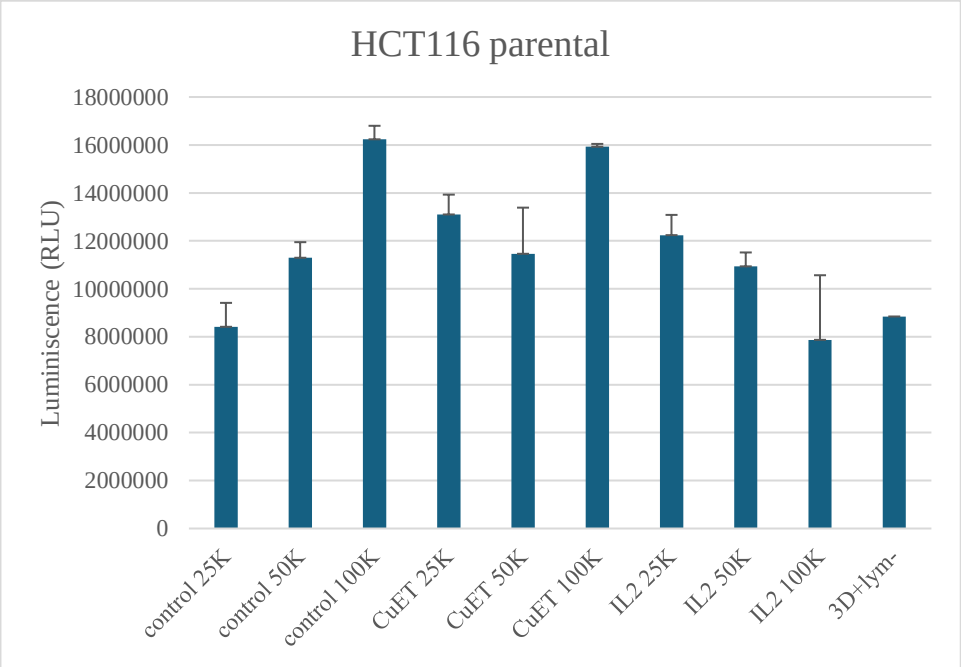

Figure 5.: Luminescence detection of ATP for evaluation of the effect of lymphocytes (control, CuET, IL-2) on HCT116 parental spheroids at different concentrations. Data are mean ±SEM.

4.1.2 Propidium Iodide Signal Intensity Analysis

Microscopic images show spheroids of the HCT116 parental line (Fig. 6), and the effect of control lymphocytes, CuET-treated lymphocytes, and IL-2-treated lymphocytes on the morphology of the spheroids. It can be observed that the spheroids incubated with the first two types of lymphocyte groups did not undergo significant morphological changes and the structure of the spheroids remained compact. However, spheroids incubated with IL-2-treated lymphocytes are characterized by disruption of the spheroid peripheral layers and visibly less compact structures. In all three groups, however, lymphocyte penetration into the deeper layers of the spheroids was not detected microscopically, suggesting integration with the spheroids primarily at their surface.

Analysis of propidium iodide staining data suggests that higher PI signal intensity correlates with higher lymphocyte concentration in the group where spheroids were treated with control lymphocytes. The highest increase in signal was observed in treatment with lymphocytes with a concentration of 100,000 cells/spheroid, then lymphocytes with a concentration of 25,000 cells/spheroid.

Spheroids treated with CuET lymphocytes of 25,000 cells/spheroid showed the lowest PI signal intensity, indicating fewer dead cells. As the concentration of CuET lymphocytes increases, the PI signal also increases, but to a lesser extent compared to the first group of control lymphocytes.

IL-2 lymphocytes provided low PI intensity at lower concentrations, and the signal increased at a concentration of 100,000 cells/spheroid, indicating toxicity at higher lymphocyte concentrations (Fig. 7).

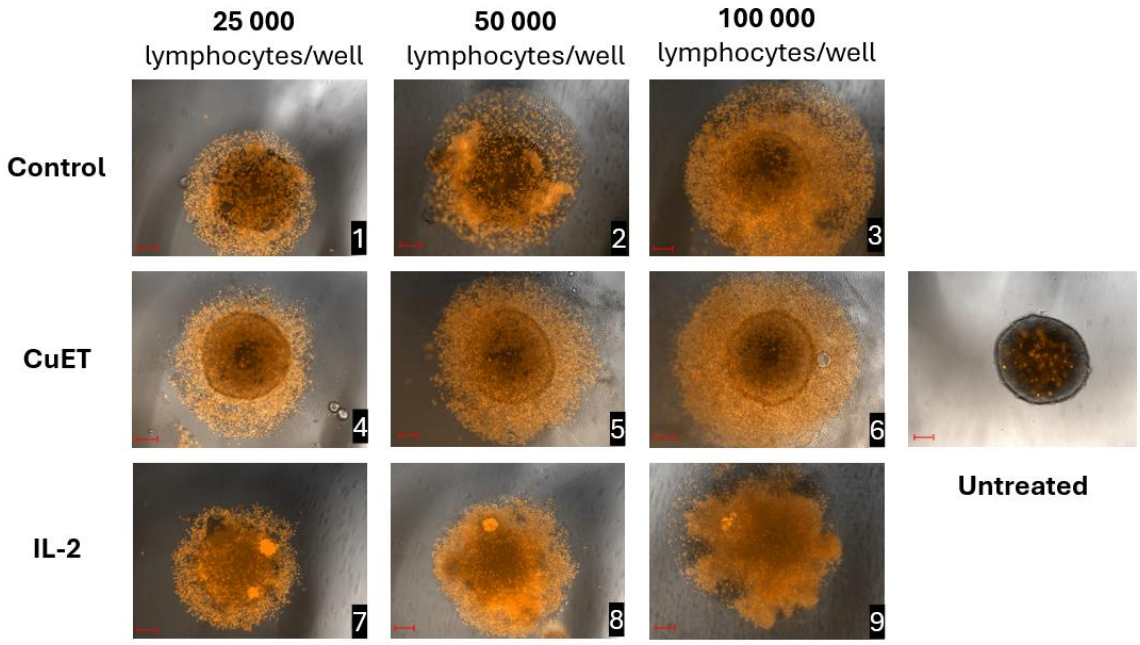

Figure 6: HCT116 parental spheroids after incubation with control, CuET, and IL-2 treated lymphocytes (propidium iodide, objective 100x, 100 µm scale bar).

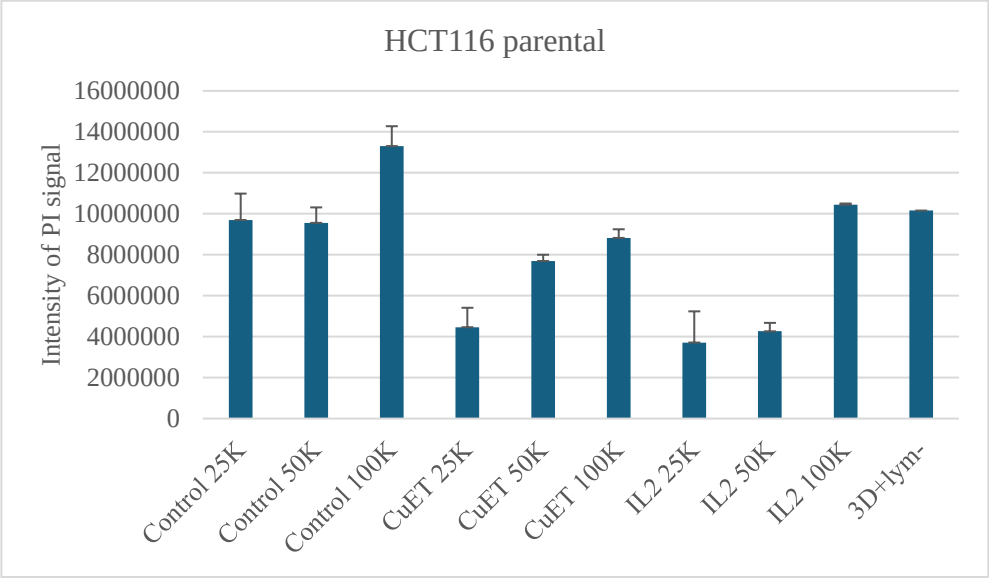

Figure 7: Evaluation of propidium iodide (PI) signal intensity for the effect of lymphocytes (control, CuET, IL-2) on HCT116 parental spheroids at different concentrations. Data are mean ±SEM.

4.1.3 Comparing Metabolic Activity and PI Signal Intensity

Comparing data from ATP luminescence analysis and PI staining for the HCT116 parental cell line provides two perspectives. Luminescence data show that lower concentrations of CuET-treated lymphocytes increase the amount of total ATP, whereas PI staining indicates low toxicity under these conditions. Furthermore, the methods agree that lymphocytes treated with IL-2 at higher concentrations have a destructive effect on spheroids. In the case of lower concentrations of IL-2 lymphocytes, we observe high ATP production by luminescence, and propidium iodide staining indicates low toxicity. The greatest difference when comparing the data can be observed in spheroids treated with the control group of lymphocytes at a concentration of 100,000 lymphocytes/spheroid.

4.2 HCT116 KRAS G13D/-

4.2.1 Quantitative Assessment of Cellular Energy

Evaluation of the ATP-detecting luminescence assay data showed that spheroids treated with the lymphocyte control group at all three concentrations resulted in reduced metabolic activity compared to control spheroids without lymphocytes (Fig. 8). There is no difference in the amount of ATP produced between the concentrations of lymphocytes acting on the spheroids.

Spheroids treated with CuET lymphocytes show decreased luminescence of 9.78 % and 14.51 % at higher lymphocyte concentrations, 50,000 and 100,000 lymphocytes/spheroid, respectively.

Treating spheroids with IL-2 lymphocytes, luminescence slightly increased at a concentration of 25,000 lymphocytes/spheroid compared to the control. Higher concentrations of lymphocytes then resulted in a decrease in the amount of ATP.

The results show that higher concentrations of IL-2 and CuET-treated lymphocytes have a negative effect on the metabolic activity of spheroids.

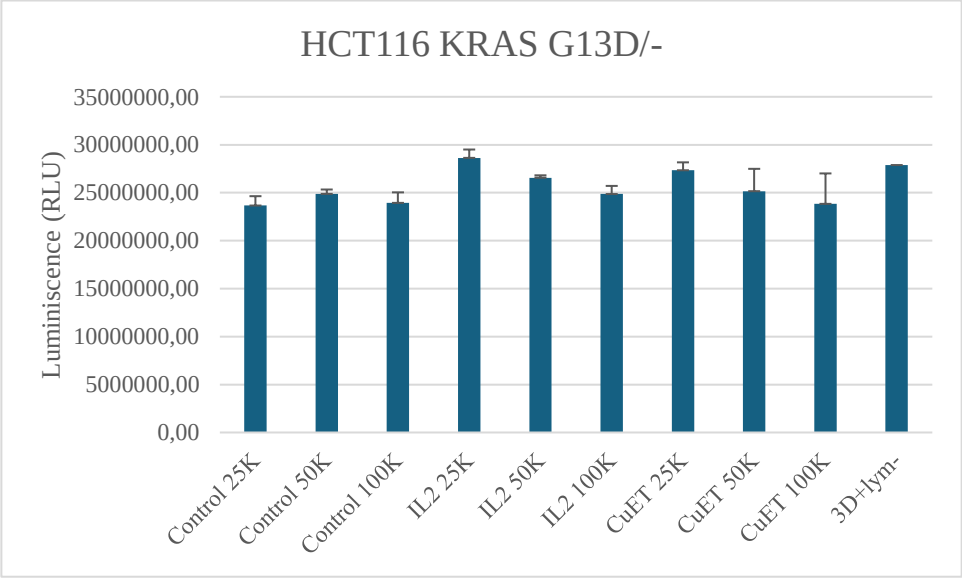

Figure 8: Luminescence detection of ATP for evaluation of the effect of lymphocytes (control, CuET, IL-2) on HCT116 KRAS G13D/- spheroids at different concentrations. Data are mean ±SEM.

4.2.2 Propidium Iodide Signal Intensity Analysis

Microscopic analysis of individual spheroids shows that the 3D models retained their integrity and structure. Interactions with lymphocytes occurred only on the surface of the spheroids and the lymphocytes could not penetrate the internal structures (Fig.9).

The data from the analysis of propidium iodide signal intensity after subtraction of the lymphocyte signal in the case of the first group of spheroids incubated with control lymphocytes show that at a concentration of 25,000 lymphocytes/spheroid, the signal is slightly higher than that of the control (3D+lym-), indicating minimal damage to the spheroids, as is the case at a concentration of 50,000 lymphocytes/spheroid. The signal is significantly increased at the highest concentration, which may indicate spheroid damage or a possible signal from lymphocytes.

The signal intensity in the case of spheroids incubated with CuET-treated lymphocytes is comparable to the control group at all three concentrations, indicating only limited damage to the spheroids (Fig. 10).

Minimal damage based on signal intensity can also be observed in spheroids incubated with IL-2 lymphocytes at the first two concentrations. At a concentration of 100,000 lymphocytes/spheroid, the signal increased significantly, similar to the control lymphocytes, suggesting some damage.

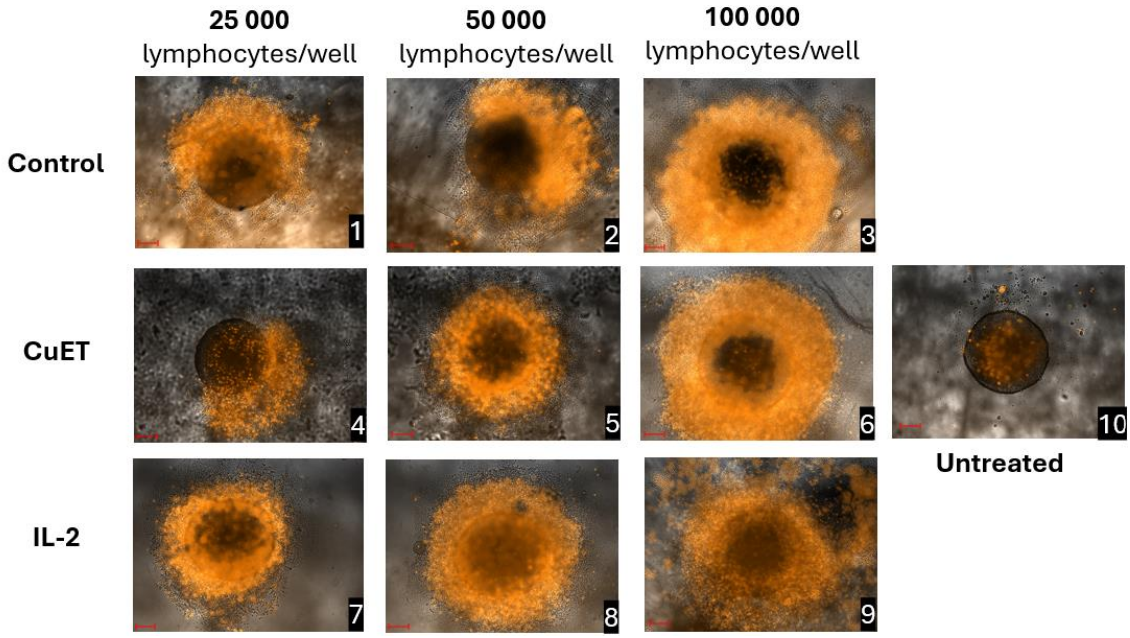

Figure 9: HCT116 KRAS G13D/- spheroids after incubation with control, CuET, and IL-2 treated lymphocytes (propidium iodide, objective 100x, 100 μm scale bar).

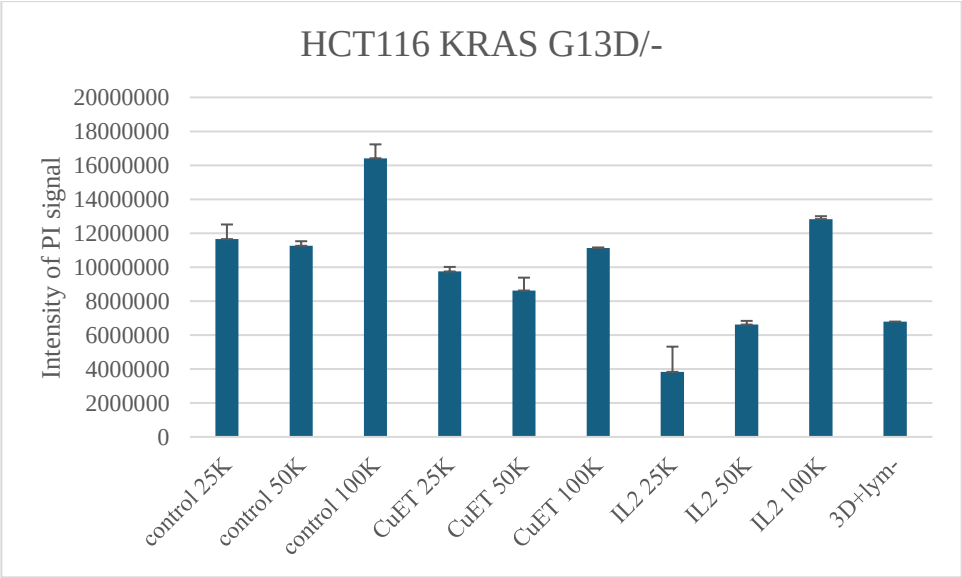

Figure 10.: Evaluation of propidium iodide (PI) signal intensity for the effect of lymphocytes (control, CuET, IL-2) on HCT116 G13D/- spheroids at different concentrations. Data are mean ±SEM.

4.2.3 Comparing Metabolic Activity and PI Signal Intensity

HCT116 KRAS G13D/- line carries a mutation in the *KRAS* gene, increasing spheroid cell resistance to various stress conditions. Data from the analysis of ATP levels by luminescence indicate relatively stable metabolic activity at both lower and higher lymphocyte concentrations. The low PI signal intensity values can be justified because most of the signal comes from dead lymphocytes. This is supported by microscopic images suggesting that the dead cells stained with propidium iodide are probably lymphocytes, not spheroid cells. According to the microscopy images taken, the integrity of the spheroid appears intact, especially the inner part, suggesting an inherent resistance of the spheroid. This idea is consistent with the fact that KRAS G13D/- mutant spheroids resist attack by immune cells.

4.3 HCT116 p53 -/-

4.3.1 Quantitative Assessment of Cellular Energy

Analysis of luminescence data (Fig. 11) from the HCT116 p53-/- line showed that spheroids treated with control lymphocytes exhibited increased luminescence with increasing lymphocyte concentration. The 3D+lym- sample served as a reference, and spheroids incubated with 25,000 lymphocytes/spheroid showed luminescence 9.35 % lower than 3D+lym-, while spheroids incubated with 50,000 and 100,000 lymphocytes/spheroid showed higher values of 9.91 % and 12.9 %, respectively. These results indicate increased metabolic activity of spheroids rather than efficient apoptosis.

When spheroids were incubated with CuET-treated lymphocytes, we observed the highest effect at a concentration of 25,000 lymphocytes/spheroid, with a 6.57% increase in luminescence compared to the control. At higher concentrations, luminescence decreased slightly.

IL-2 lymphocyte-treated spheroids had the lowest luminescence values across all concentrations, with the lowest value recorded at 25,000 lymphocytes/spheroid, suggesting potential toxicity, particularly at lower concentrations.

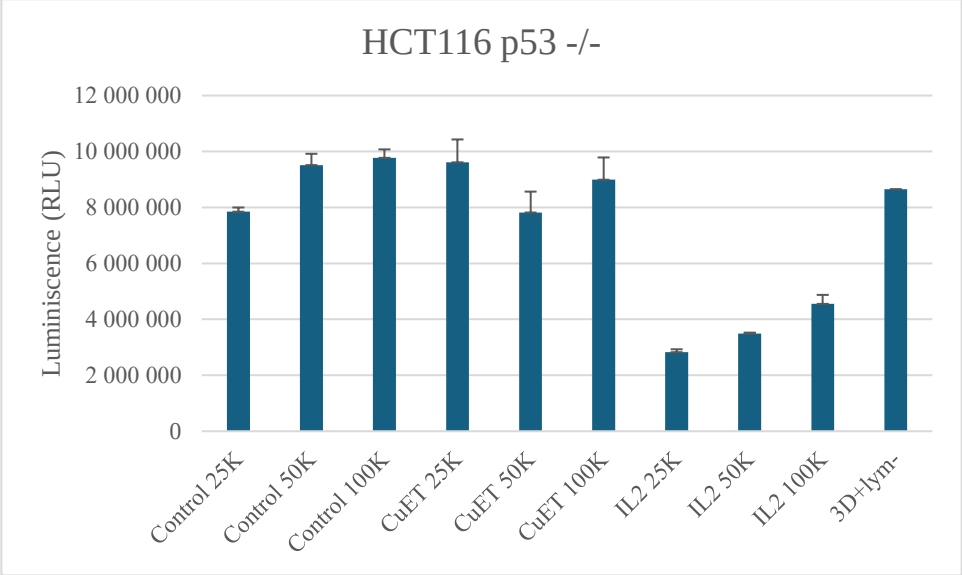

Figure 11.: Luminescence detection of ATP for evaluation of the effect of lymphocytes (control, CuET, IL-2) on HCT116 KRAS G13D/- spheroids at different concentrations. Data are mean ±SEM.

4.3.2 Propidium Iodide Signal Intensity Analysis

Microscopic examination of the spheroids (Fig. 12) shows that, as in the previous lineage, they maintained their integrity and structure in most cases. In particular, in the third test group and at concentrations of 50,000 and 100,000 lymphocytes/spheroid, the most intense and diffuse fluorescence signal can be observed, indicating increased damage.

When the signal intensity of propidium iodide was analyzed in spheroids incubated with control lymphocytes at a concentration of 25,000 lymphocytes/spheroid, the signal increased by 12 % compared to the reference sample (Fig. 13). At a concentration of 50,000 lymphocytes/spheroid, the signal decreased by only 5 % and was slightly higher at a concentration of 100,000 lymphocytes/spheroid. Generally, the signal in the control group is only slightly higher than the 3D+lym- values, suggesting that control lymphocytes damage the spheroids, but the effect is insignificant.

In the case of spheroids incubated with CuET-treated lymphocytes, we observe a trend of increasing PI signal intensity with increasing lymphocyte concentration, where at a concentration of 100,000 lymphocytes/spheroid, it is even 93, 86 % higher compared to the control, indicating cytotoxic effects of CuET-treated lymphocytes.

The third test group shows the same trend as the second group, i.e. increasing PI signal with increasing lymphocyte concentration. However, the lowest concentration of 25,000 lymphocytes/spheroid caused minimal spheroid damage and decreased signal intensity compared to the control.

According to the analysis of signal intensity data, it can be said that the type and concentration of lymphocytes highly influence the degree of spheroid damage, with CuET and IL-2 showing a particularly strong effect at high concentrations.

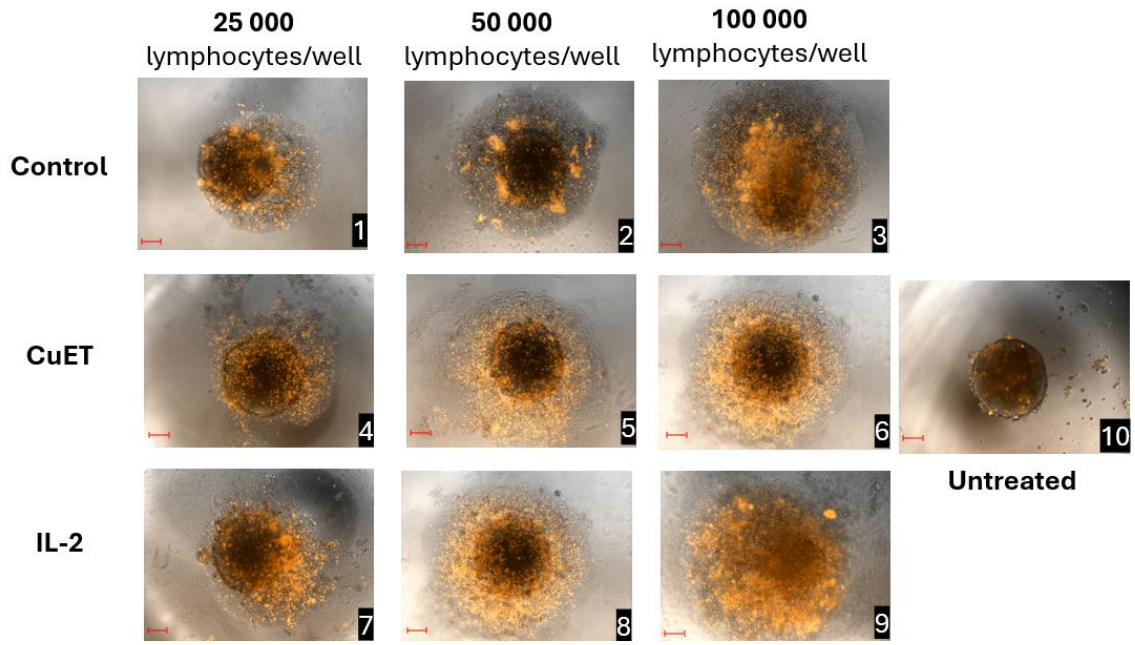

Figure 12: HCT116 p53 -/- spheroids after incubation with control, CuET, and IL-2 treated lymphocytes (propidium iodide, objective 100x, 100 µm scale bar).

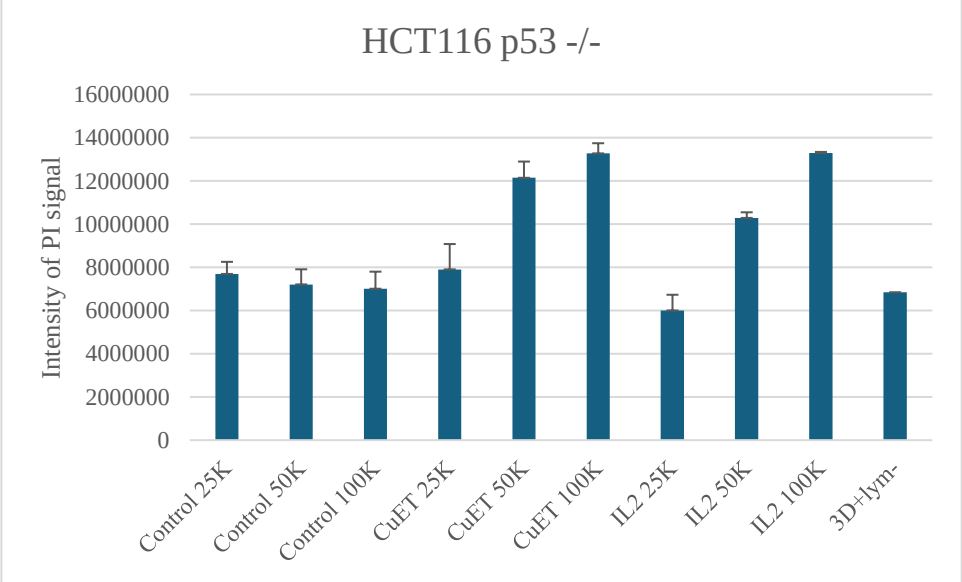

Figure 13: Evaluation of propidium iodide (PI) signal intensity for the effect of lymphocytes (control, CuET, IL-2) on HCT116 p53-/- spheroids at different concentrations. Data are mean ±SEM.

4.3.3 Comparing Metabolic Activity and PI Signal Intensity

Analysis of the luminescence essay and PI signal intensity shows a consensus that at a concentration of 25,000 lymphocytes/spheroid in the first group, lymphocytes interact with spheroids and influence their metabolic activity. In contrast, at higher concentrations, their influence decreases. The data also agree spheroids have high metabolic activity and low PI signal at a concentration of 25,000 lymphocytes/spheroid in the CuET group. Spheroid damage is more pronounced in the IL-2-treated lymphocyte group at higher concentrations.

An irregularity occurs with the PI signal of IL-2 at 25,000 lymphocytes/spheroid, which is lower than that of the reference control, whereas ATP analysis shows higher metabolism. This suggests a possible error in the background lymphocyte readout. The absence of p53 in the spheroid lineage leads to a limited ability to trigger apoptosis, which explains the high metabolic activity (ATP) even in the presence of cell damage (PI signal). Fig.12 is consistent with most of the data from ATP and PI analyses.

4.4 HCT116 p53 +/-

4.4.1 Quantitative Assessment of Cellular Energy

Another tested line was the HCT116 p53 +/- line. Within the spheroids incubated with control lymphocytes, a decreasing level of ATP is observed, which may be caused by greater activity of lymphocytes at higher concentrations against this line, leading to a reduction in ATP (Fig.14).

In the second group of spheroids, which was incubated with CuET-treated lymphocytes, a similar trend is observed in the first group, i.e., decreasing ATP with increasing concentration. However, compared to the control (3D+lym-), there is a higher amount of ATP, so it can be assumed spheroids had increased activity during incubation with lymphocytes.

The third group of spheroids, which was incubated with IL-2-treated lymphocytes, showed the most significant reduction in the amount of ATP, with the lowest amount of ATP recorded at a concentration of 100,000 lymphocytes per spheroid. This result suggests that IL-2 significantly stimulates the cytotoxic activity of lymphocytes against spheroids, making them more harmful and reducing their viability.

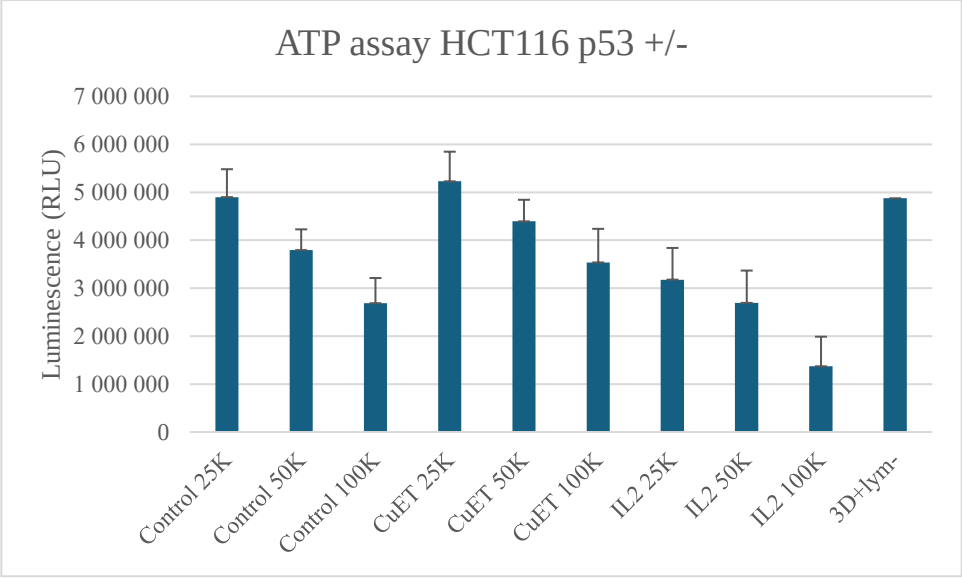

Figure 14: Luminescence detection of ATP for evaluation of the effect of lymphocytes (control, CuET, IL-2) on HCT116 p53 +/- spheroids at different concentrations. Data are mean ±SEM.

4.4.2 Propidium Iodide Signal Intensity Analysis

Based on the evaluation of microscopic images of the HCT116 p53 +/- line, after incubation with spheroids in the control group, it can be observed that neither concentration of lymphocytes disrupted the spheroids, with their structural integrity was preserved (Fig.15). At a concentration of 100,000 lymphocytes/spheroids this is not so clear, but the core of the spheroid can still be observed.

The integrity of the CuET lymphocytes incubated with spheroids is intact in all three cases - the intact spheroid margins can be observed nicely, even at the highest concentration.

According to microscopic images, the IL-2 group of lymphocytes had the most intense effect on the spheroids, specifically at concentrations of 50,000 and 100,000 lymphocytes/spheroid. The integrity was no longer preserved and could penetrate the spheroid's core.

Quantitative analysis of signal intensity in the first test group when spheroids were incubated with control lymphocytes showed that all three groups showed increased PI signal intensity compared to control, with the highest signal intensity at a concentration of 50,000 lymphocytes/spheroid (Fig.16).

In the second group, when spheroids were incubated with CuET-treated lymphocytes, the highest signal intensity was again observed at a concentration of 50,000 lymphocytes/spheroid. Of all the groups tested, the signal increase was highest in this group of lymphocytes; this suggests a strong cytotoxic effect of CuET against HCT116 p53 +/- spheroids.

As in the two previous groups, the signal intensity was highest in the IL-2-treated group at a concentration of 50,000 lymphocytes/spheroid.

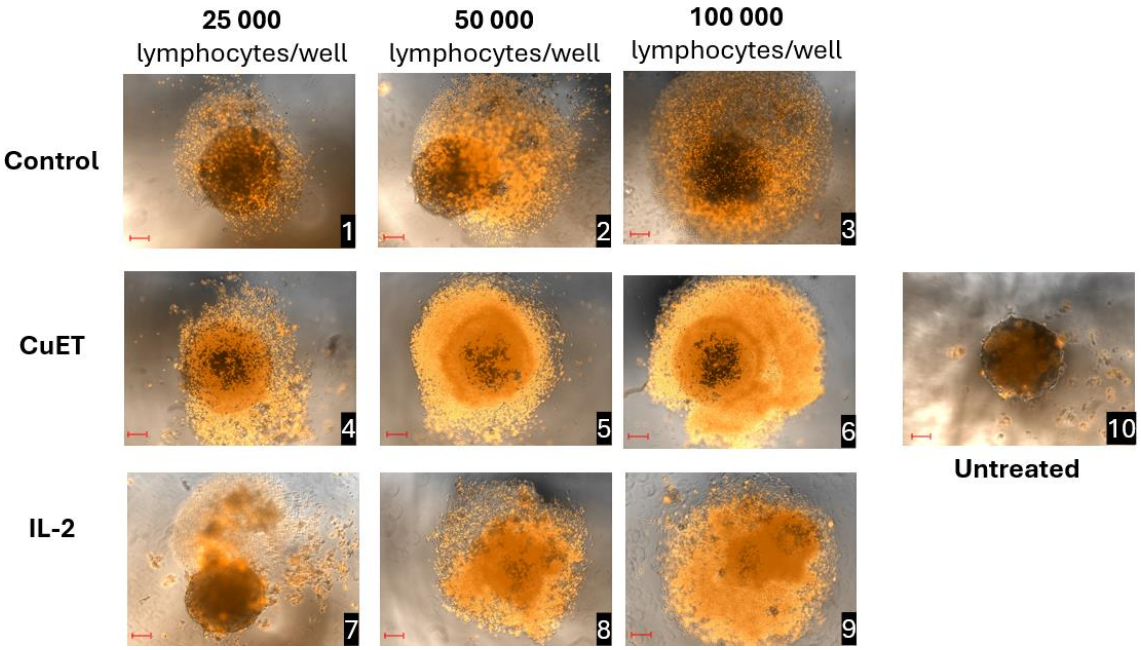

Figure 15: HCT116 p53 +/- spheroids after incubation with control, CuET, and IL-2 treated lymphocytes (propidium iodide, objective 100x, 100 µm scale bar).

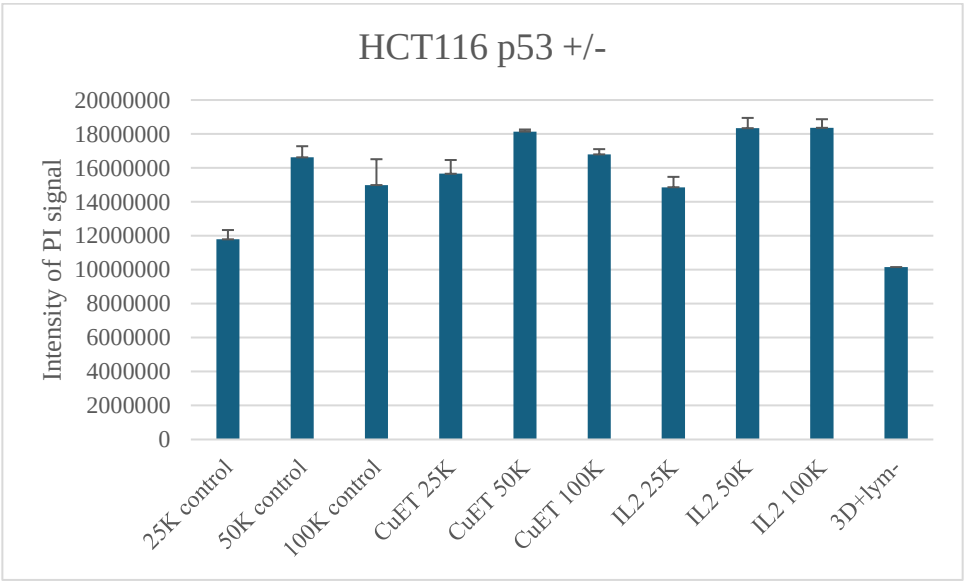

Figure 16: Evaluation of propidium iodide (PI) signal intensity for the effect of lymphocytes (control, CuET, IL-2) on HCT116 p53 +/- spheroids at different concentrations. Data are mean ±SEM.

4.4.3 Comparing Metabolic Activity and PI Signal Intensity

Comparison of the data from the analysis of ATP amount, PI signal intensity, and microscopic image of HCT116 p53 +/- spheroids will provide a more comprehensive view of the whole experiment. We can see that the methods agree that concentrations of 50,000 and 100,000 IL-2 lymphocytes/spheroid significantly induce cytotoxicity. This is confirmed by microscopic images, where the spheroids' integrity was no longer preserved at the concentrations mentioned.

However, the data are variable in the CuET lymphocyte group, where ATP luminescence shows a slight decrease, but the intensity of the PI signal is significantly increased here (+78.6 %). We also observe variability when using control lymphocytes, with an increase in PI (+45.57 %) and a decrease in ATP (-67.2 %).

The experimental results suggest that despite the potential lineage resistance associated with the loss of one p53 allele, lymphocytes can effectively induce spheroid death, especially IL-2-treated lymphocytes.

4.5 HCT116 KRAS +/-

4.5.1 Quantitative Assessment of Cellular Energy

Another line tested was HCT116 KRAS +/- (Fig.17), which showed unexpected results when interacting with lymphocytes. According to the hypothesis, the line should be more resistant to the action of lymphocytes. However, across all three groups tested observed, an unusual phenomenon was observed - the lowest concentrations (25,000 lymphocytes/spheroid) appeared to be the most potent, i.e., the spheroids produced the least amount of ATP. High concentrations (100,000 lymphocytes/spheroid) showed the same amount of ATP as the 3D+lym- control, i.e., untreated spheroid.

Thus, it is possible that in the case of the HCT116 KRAS+/- line, lower concentrations of lymphocytes are more efficient, and higher concentrations of lymphocytes may lead to, for example, triggering mechanisms that protect spheroids from destruction.

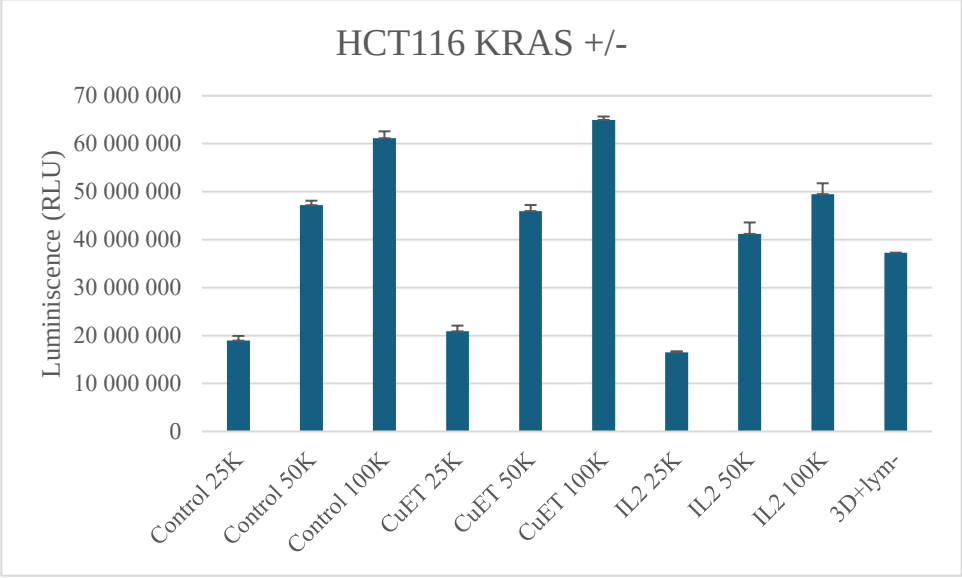

Figure 17.: Luminescence detection of ATP for evaluation of the effect of lymphocytes (control, CuET, IL-2) on HCT116 KRAS +/- spheroids at different concentrations. Data are mean ±SEM.

4.5.2 Propidium Iodide Signal Intensity Analysis

In HCT116 KRAS +/- spheroids, microscopic images show that the first two test groups of lymphocytes (control and CuEt lymphocytes) did not damage the integrity of the spheroids, and their structure was preserved even at high concentrations (Fig. 18). On the other hand, spheroids incubated with IL-2 lymphocytes showed a broken structure according to the images, indicating that these lymphocytes have the highest cytotoxic effect against the test line.

Signal intensity analysis after treatment of spheroids with control lymphocytes showed a similar increase in signal when incubated with 50,000 and 100,000 lymphocytes/spheroids, by 46.14 and 46.80 %, respectively (Fig.19). This suggests that even normal lymphocytes strongly affect this spheroid lineage.

In the second test group, the highest increase in PI signal occurred at a concentration of 50,000 lymphocytes/spheroid. At a concentration of 100,000 lymphocytes/spheroid, contrary to expectation, there appeared to be a decrease in lymphocyte toxicity.

Quantitative analysis of the IL-2-treated lymphocyte group is the most effective. Here, the increase in PI signal was highest across groups.

Data analysis for HCT116 KRAS +/- spheroids showed that stimulation of lymphocytes with IL-2 and CuET could effectively enhance their toxicity to tumor cells, suggesting the potential of these methods in treating tumors with genetic mutations such as KRAS.

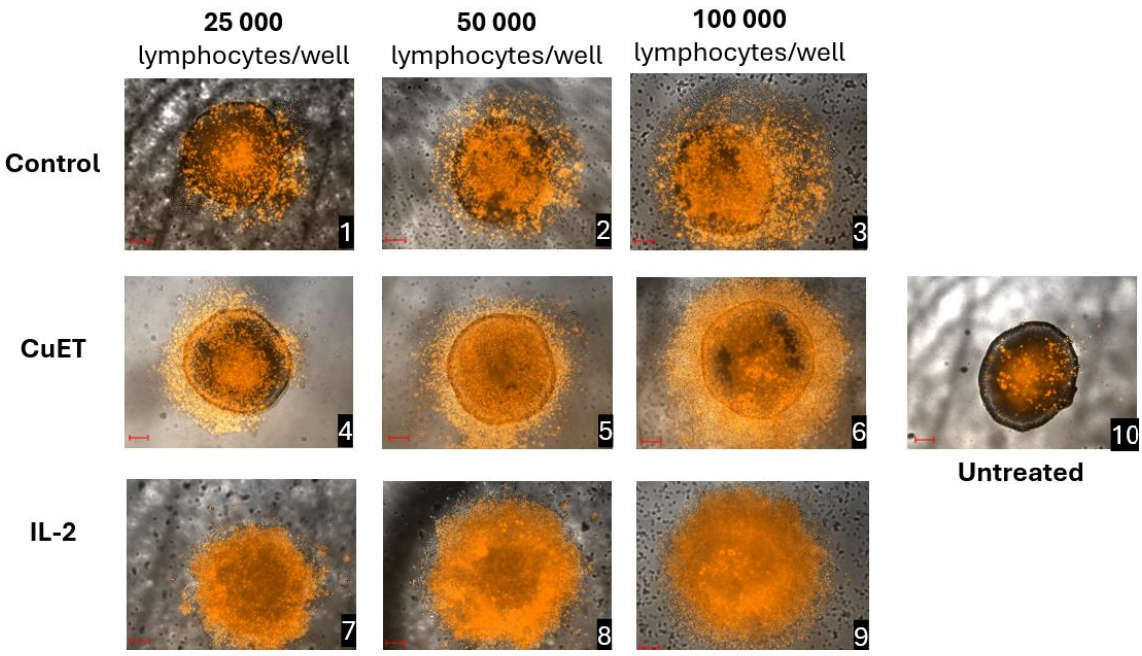

Figure 18: HCT116 KRAS +/- spheroids after incubation with control, CuET, and IL-2 treated lymphocytes (propidium iodide, objective 100x, 100 µm scale bar).

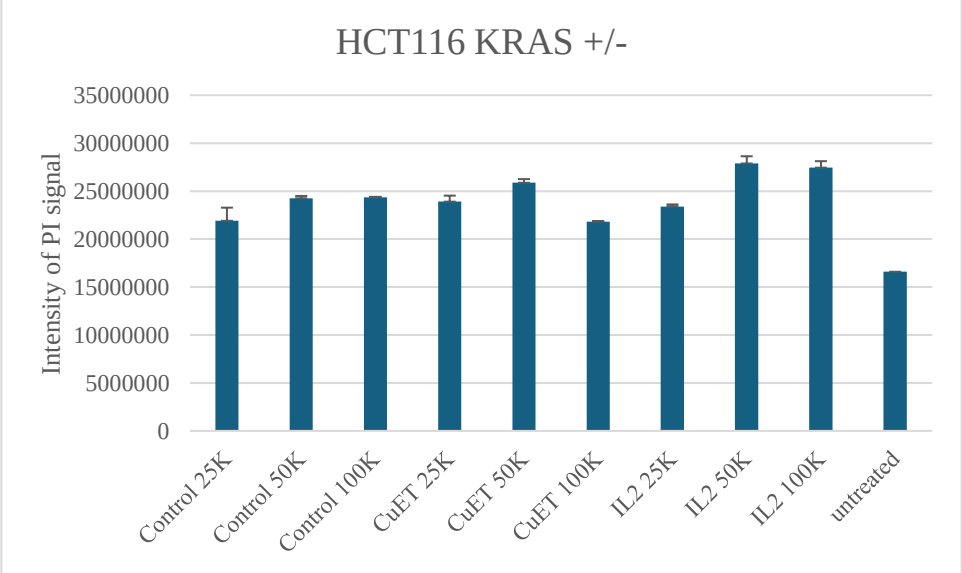

Figure 19.: Evaluation of propidium iodide (PI) signal intensity for the effect of lymphocytes (control, CuET, IL-2) on HCT116 KRAS +/- spheroids at different concentrations. Data are mean ±SEM.

4.5.3 Comparing Metabolic Activity and PI Signal Intensity

When comparing the results of both methods, we observe agreement in the induction of cytotoxicity at higher concentrations of IL-2 lymphocytes. In both data types, cell damage is observed with increasing lymphocyte numbers. ATP data slightly decrease, while PI data show an increased signal. This is indicative of the efficiency of IL-2 lymphocytes, which can be confirmed by microscopic images of spheroids of the HCT116 KRAS +/- line.

The differences in the data are evident in the control and CuET lymphocyte groups at low and medium concentrations, where, for example, we see significant differences in the amount of ATP in the control group. In contrast, the PI data are rather consistent.

The agreement and differences in the data highlight the importance of comprehensively using multiple methods to assess cytotoxicity in biomedical research.

4.6 HCT116 R248 w/-

4.6.1 Quantitative Assessment of Cellular Energy

The last tested line was HCT116 R248 w/-, where, in the first test group, there was an increase in ATP across the concentrations used compared to the control, most significantly at the lowest concentration of 25 000 lymphocytes/spheroid, 17.8% (Fig.20). The increase was not as marked at other concentrations, indicating a general stimulatory or non-inhibitory effect of control lymphocytes on the spheroids.

In the second test group, there was no significant increase or decrease in the amount of ATP in the spheroids compared to the control, and the CuET-treated lymphocyte group had neither a stimulatory nor a toxic effect on spheroid viability. Only highest concentration of lymphocytes was able to slightly decrease ATP levels.

The same phenomenon as in the second test group was observed after incubation of spheroids with IL-2 treated lymphocytes, where a significant decrease or increase in ATP levels compared to the control is not observed.

Based on quantitative analysis of the luminescence essay data, this mutation at codon 248 leads to spheroids' resistance to the lymphocytes' potential cytotoxic effect.

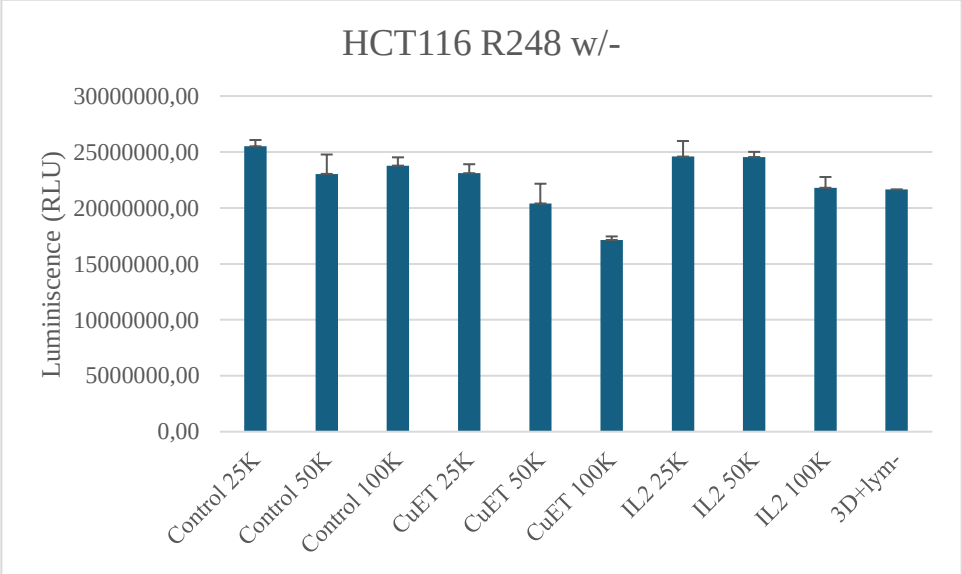

Figure 20.: Luminescence detection of ATP for evaluation of the effect of lymphocytes (control, CuET, IL-2) on HCT116 R248 w/- spheroids at different concentrations. Data are mean ±SEM.

4.6.2 Propidium Iodide Signal Intensity Analysis

Microscopic images of the HCT116 R248 w/- line show that spheroid integrity was preserved in all three groups of lymphocytes incubated with spheroids (Fig.21). The core and margins of the spheroids can be observed to be intact. Thus, penetration of lymphocytes into the core of the spheroid itself does not appear to have occurred in either case.

At a concentration of 25,000 control lymphocytes/spheroid (Fig. 22), there was a decrease in signal compared to the control, indicating that the number of lymphocytes is not sufficient for efficient destruction of the spheroid cells. At a concentration of 50,000 lymphocytes/spheroids there was a clear increase in signal (+27.6%) and the highest increase in signal was observed at a concentration of 100,000 lymphocytes/spheroid, indicating a high ability of lymphocytes to destroy spheroid cells.

CuET-treated spheroids responded similarly to the control group, with a concentration of 50, 000 lymphocytes/well appearing more effective than the control group. A significant increase in signal was observed at the highest concentration of 100,000 lymphocytes/spheroid (132%).

A similar trend was observed in the last group tested when spheroids were incubated with IL-2-stimulated lymphocytes. At a concentration of 50,000 lymphocytes, the increase was similar to that of CuET-treated lymphocytes; at a concentration of 100,000 lymphocytes, this concentration again led to increased cytotoxicity.

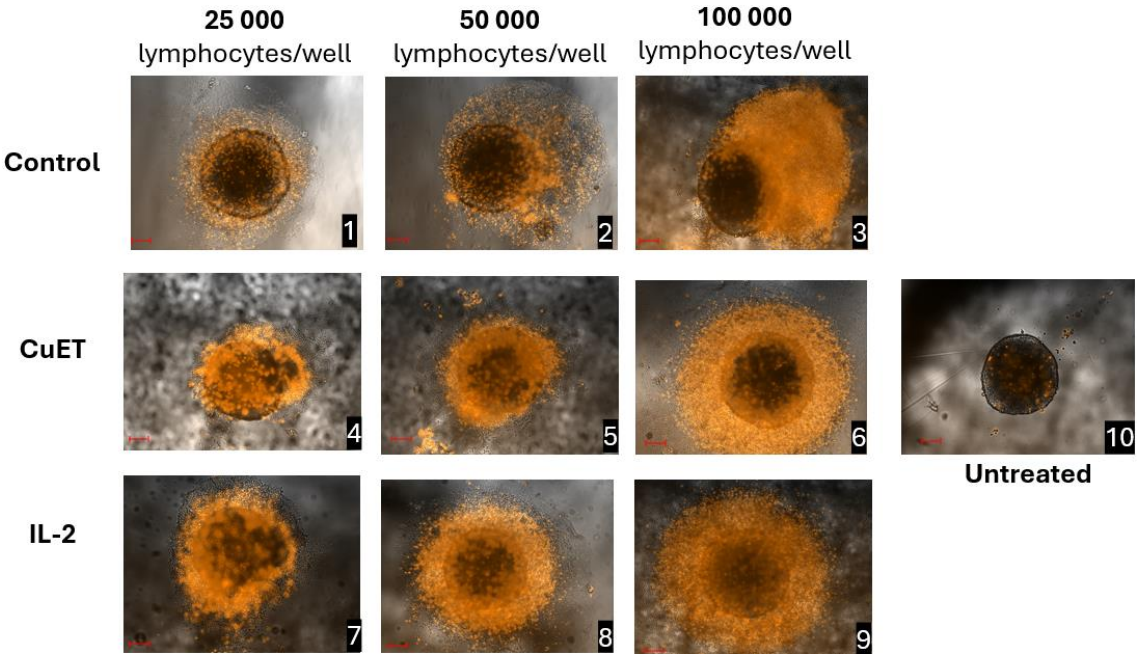

Figure 21: HCT116 R248 w/- spheroids after incubation with control, CuET, and IL-2 treated lymphocytes (propidium iodide, objective 100x, 100 µm scale bar).

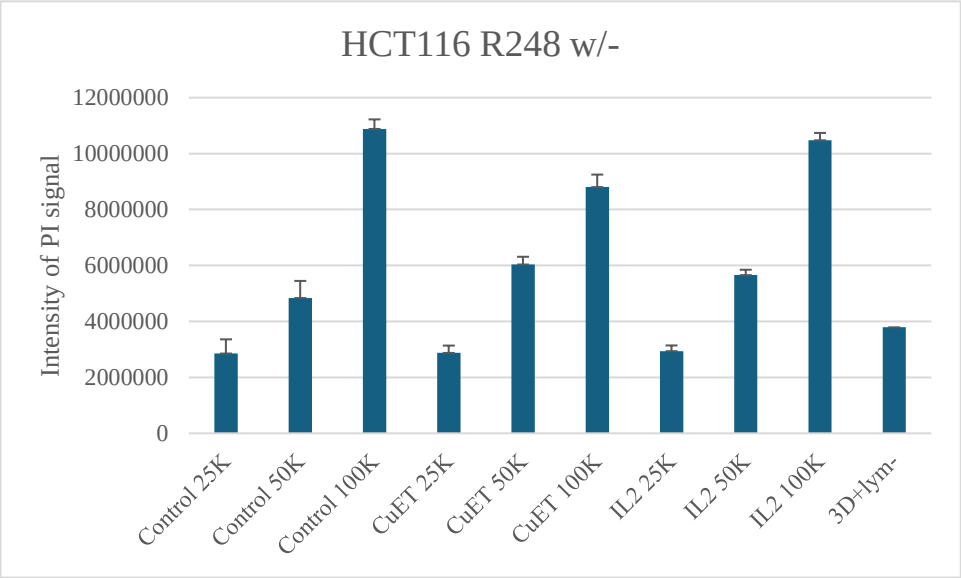

Figure 22: Evaluation of propidium iodide (PI) signal intensity for the effect of lymphocytes (control, CuET, IL-2) on HCT116 R248 w/- spheroids at different concentrations. Data are mean ±SEM.

4.6.3 Comparing Metabolic Activity and PI Signal Intensity

A comparison of the luminescence and PI signal intensity data shows that in the control group, ATP values decrease and PI signal increases with increasing lymphocyte concentration, which correlates with each other. The same trend can be observed in the CuET and IL-2 treated lymphocyte groups; here, too, ATP slightly decreases and PI signal increases in spheroids.

While both methods show similar patterns, each shows them to a different degree - the differences in the ATP decrease are not as apparent for luminescence. For the PI signal, the differences between the concentrations are already wider. According to the HCT116 R248 w/- line characteristics, increased resistance was expected, which, according to the data, could be consistent with the results from the ATP amount measurements. However, both methods provide a different perspective on the cellular state.

4.8 Synergy studies

According to the diploma thesis by Vrablíková, 2022 the drugs 5-fluorouracil, cisplatin, and irinotecan exhibit a synergistic effect in certain ratio combinations. However, this effect must be demonstrated at the protein level. The levels of acetyl-α-tubulin (Ac-α-tubulin) were first monitored using Western blot (Fig.23). Acetyl-α-tubulin is associated with long-lasting, stabilized microtubules, and the chemotherapeutics used in this work do not have a direct effect on α-tubulin acetylation (L. Li & Yang, 2015).

Spheroids composed of HCT116 cells showed a strong decrease in ac-α-tubulin levels after treatment with 5-FU: cisplatin 1:1, indicating significant microtubule destabilization. In contrast, the combination 5-FU: cisplatin 1:2 led to a strong increase in signal compared to the untreated control, which may reflect treatment-induced microtubule stabilization. The irinotecan: cisplatin 4:1 combination resulted in a slight decrease in band intensity relative to control.

In 7:3 cocultures of HCT116 and CCD18-Co cells, treatment with 5-FU: cisplatin 1:2 did not induce significant changes in ac-α-tubulin levels, suggesting that microtubules remained stable. However, a marked decrease was observed after treatment with irinotecan: cisplatin 4:1, indicating the sensitivity of this coculture model to irinotecan.

In 3:7 cocultures, treatment with 5-FU: cisplatin 1:1 caused a pronounced reduction in ac-α-tubulin expression. In contrast, the irinotecan: cisplatin 4:1 combination resulted in a moderate decrease, approximately half the level of the untreated control. This coculture, predominately of fibroblasts, appears to be particularly sensitive to treatment, especially to 5-FU: cisplatin 1:1.

Spheroids composed of CCD18-Co fibroblasts showed high stabilization of ac-α-tubulin levels following 5-FU: cisplatin 1:2 treatment. In contrast, other drug combinations led to a substantial decrease in signal.

Overall, the 5-FU: cisplatin 1:1 combination significantly reduced ac-α-tubulin levels across all tested models and appears to be the most cytotoxic. The 1:2 combination caused an increase in ac-α-tubulin levels in monocultures, suggesting microtubule stability. In the 7:3 coculture, this combination had minimal effect, while irinotecan: cisplatin 4:1 caused a strong decrease in both the 7:3 coculture and the CCD18-Co monoculture.

Figure 23: Western blot analysis of Ac-α-tubulin (52 kDa) in different 3D cultures after 7-day treatment with different drug ratios. . **1** – HCT116 *untreated*; **2** – HCT116 treated with *5-fluorouracil:cisplatin 1:1*; **3** – HCT116 treated with *5-fluorouracil:cisplatin 1:2*; **4** – HCT116 treated with *irinotecan:cisplatin 4:1*; **5** – HCT116:CCD18-Co 7:3 *untreated*; **6** - HCT116:CCD18-Co 7:3 treated with *5-fluorouracil:cisplatin 1:2*; **7** - HCT116:CCD18-Co 7:3 treated with *irinotecan:cisplatin 4:1*; **8** - HCT116:CCD18-Co 3:7 *untreated*, **9** - HCT116:CCD18-Co 3:7 treated with *5-fluorouracil:cisplatin 1:1*; **10** - HCT116:CCD18-Co 3:7 treated with *irinotecan:cisplatin 4:1*; **11** – CCD18-Co *untreated*; **12** – CCD18-Co treated with *5-fluorouracil:cisplatin 1:1*; **13** – CCD18-Co treated with *5-fluorouracil:cisplatin 1:2*; **14** – CCD18-Co treated with *irinotecan:cisplatin 4:1*.

The next part of the western blot analysis was focused on the detection of p21, a cell cycle-regulating protein based on the inhibition of cyclin-dependent kinase (CDK) and playing a key role in stopping cell division in response to DNA damage or stress (Fig.24).

In spheroids composed of HCT116 cells, a significant increase in p21 expression was observed after treatment with 5-fluorouracil: cisplatin at a ratio of 1:1, as well as after treatment with irinotecan: cisplatin 4:1, which resulted in the highest p21 levels recorded. The response to 5-fluorouracil: cisplatin 1:2 was more moderate, with only a partial increase in protein abundance.

In the 7:3 HCT116:CCD18-Co co-culture, strong induction of p21 was observed after treatment with 5-fluorouracil: cisplatin 1:2, while the most pronounced increase among all samples was again recorded following irinotecan: cisplatin 4:1. This could be attributed to the possible involvement of fibroblasts in the stress response.

In the 3:7 co-culture model, increased p21 expression was also observed after irinotecan: cisplatin 4:1 treatment compared to the untreated control, while the 5-fluorouracil: cisplatin 1:1 combination had a more negligible, though still noticeable, effect.

In spheroids composed of CCD18-Co fibroblasts, the combination of irinotecan: cisplatin 4:1 once again resulted in the strongest induction of p21, while the other drug combinations led only to minor increases.

Among the drug regimens tested, irinotecan: cisplatin 4:1 appeared to be the most effective, causing the largest increase in p21 expression across the models. The combination of 5-fluorouracil: cisplatin 1:1 induced a strong response, particularly in HCT116 cells, while the 1:2 ratio showed a weaker but still evident effect.

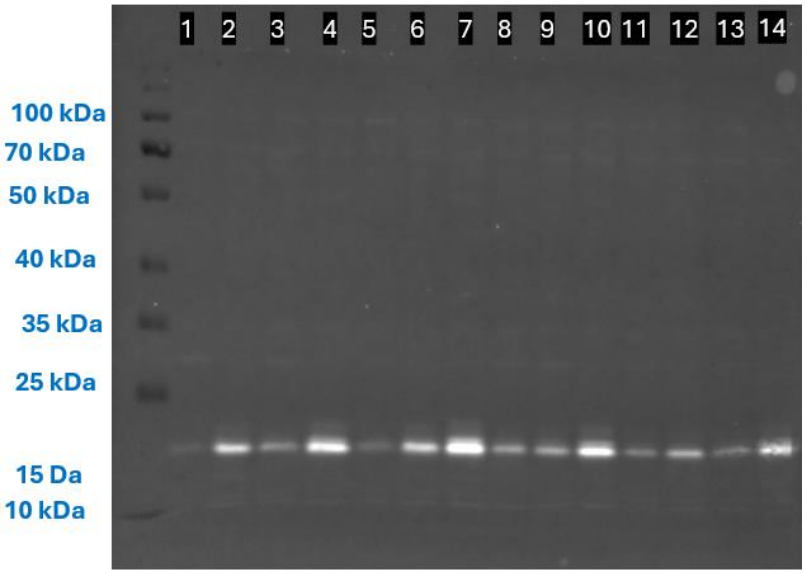

Figure 24: Western blot analysis of p21 (21 kDa) in different 3D cultures after 7-day treatment with different drug ratios. **1** – HCT116 *untreated*; **2** – HCT116 treated with *5-fluorouracil:cisplatin 1:1*; **3** – HCT116 treated with *5-fluorouracil:cisplatin 1:2*; **4** – HCT116 treated with *irinotecan:cisplatin 4:1*; **5** – HCT116:CCD18-Co 7:3 *untreated*; **6** - HCT116:CCD18-Co 7:3 treated with *5-fluorouracil:cisplatin 1:2*; **7** - HCT116:CCD18-Co 7:3 treated with *irinotecan:cisplatin 4:1*; **8** - HCT116:CCD18-Co 3:7 *untreated*, **9** - HCT116:CCD18-Co 3:7 treated with *5-fluorouracil:cisplatin 1:1*; **10** - HCT116:CCD18-Co 3:7 treated with *irinotecan:cisplatin 4:1*; **11** – CCD18-Co *untreated*; **12** – CCD18-Co treated with *5-fluorouracil:cisplatin 1:1*; **13** – CCD18-Co treated with *5-fluorouracil:cisplatin 1:2*; **14** – CCD18-Co treated with *irinotecan:cisplatin 4:1*.

A comparison of p21 and ac-α-tubulin levels revealed an inverse relationship between microtubule stability and stress response activation. The combinations of 5-fluorouracil: cisplatin 1:1 and irinotecan: cisplatin 4:1 most frequently led to increased p21 expression and a concurrent reduction in ac-α-tubulin levels, suggesting cytotoxic effects and the activation of apoptotic or DNA repair pathways. In contrast, the 1:2 combination was associated with preserved microtubule stability and a low level of stress response.

5 Discussion

In this thesis, the spheroid formation method described by Das et al., 2015 was used, which employs agarose-coated plates for spheroid generation. This method is simple, fast, easily replicable, cost-effective, and potentially used in high-throughput screening.

The first part of the thesis focused on the HCT116 parental colorectal cancer cell line and its six mutant variants, from which uniform spheroids of 5,000 cells per well were successfully generated. These spheroids were subsequently incubated with three groups of lymphocytes – control lymphocytes, CuET-treated lymphocytes, and IL-2-treated lymphocytes – at three different concentrations. The effect of lymphocytes on spheroids was evaluated after three days using fluorescence microscopy (measuring PI intensity) and luminescence analysis (measuring ATP levels).

According to the hypothesis, increasing lymphocyte concentration was expected to decrease ATP levels and a corresponding increase in PI signal. Different results were anticipated for more resistant cell lines, such as HCT116 KRAS +/-.

Different cell lines responded differently to the treatment. The first tested line, HCT116 parental, showed increased metabolic activity at low lymphocyte concentrations. At higher concentrations, IL-2 led to the disruption of spheroid integrity and increased cytotoxicity. The parental line exhibited moderate sensitivity to CuET- and IL-2-treated lymphocytes.

The HCT116 G13D/- line had low metabolic activity across all lymphocyte concentrations. Control and CuET-treated lymphocytes caused minimal damage to spheroids, while IL-2 exhibited cytotoxic effects at high concentrations. This line demonstrated high resistance to treatment.

HCT116 p53 -/- showed high metabolic activity, suggesting that the cells resist apoptosis due to the absence of the p53 gene (Labuschagne et al., 2018). The HCT116 p53 +/- line decreased ATP levels with increasing lymphocyte concentration, and PI analysis revealed a significant cytotoxic effect in spheroids incubated with CuET- and IL-2-treated lymphocytes. This line was more sensitive than HCT116 p53 -/- but still more resistant than the HCT116 parental line.

An unexpected trend was observed in HCT116 KRAS +/-. Although the KRAS mutation was expected to increase resistance to lymphocytes, ATP levels increased with higher lymphocyte concentrations. However, the PI signal evaluation provided more consistent results. The methods agreed on the cytotoxic effect of IL-2, which was further supported by microscopic images.

The last tested line, HCT116 R248 w/-, did not show significant ATP decreases, consistent with its mutation, specifically the p53 knockout at codon 248. However, these results did not fully align with PI intensity data. Nevertheless, microscopic images confirmed that the spheroid structure remained intact.

Based on the evaluation of the results of individual methods, it can be said that IL-2-treated lymphocytes were more effective than CuET-treated lymphocytes, especially against lines with functional or partially functional p53.

CellTiter-Glo® 3D Cell Viability Assay is widely used for assessing spheroid viability (Kijanska & Kelm, 2016). However, in this thesis, it did not always provide consistent and hypothesis-based results. Although the ATP signal of non-incubated lymphocytes was measured and subsequently subtracted, this procedure may not be entirely sufficient. For a more accurate determination of spheroid viability, it would be more appropriate to remove lymphocytes before the analysis itself, for example by washing/filtrating the spheroids or centrifuging them.

Like the assessment of spheroid metabolic activity, fluorescence microscopy combined with PI signal intensity measurement has limitations. The results can be distorted by the presence of lymphocytes, even after their subsequent subtraction. However, microscopy provides significant added value by visually assessing the spheroids, their structure and integrity. This allows assessment of whether the spheroids have been physically disrupted, providing a more comprehensive view of the effect of lymphocytes.

Based on the diploma thesis Vrablíková, 2022, ratio combinations of the drugs 5-fluorouracil, cisplatin, and irinotecan were selected that could demonstrate a synergistic effect. This effect had to be verified at the molecular level.

In this thesis, changes in the levels of the proteins ac-α-tubulin and p21 were monitored following a seven-day treatment with combinations of the aforementioned

chemotherapeutic agents in spheroids composed of HCT116 cells, CCD18-Co fibroblasts and co-cultures in 7:3 and 3:7 ratios. The results indicate varying sensitivity among the different models, influenced by distinct mechanisms of response to treatment and by the associated tumor microenvironment.

Levels of p21, a marker of the cellular stress response, increased most significantly after treatment with irinotecan and cisplatin at a 4:1 ratio across all spheroid models. The highest increase in p21 abundance was observed in the 7:3 co-culture, likely reflecting the combined effect of tumor cells and fibroblasts. Based on the literature (Ortiz-Otero et al., 2020), it was initially assumed that fibroblasts would enhance tumor resistance; however, this was not the case for the tested cell line. An increase in p21 levels was also observed in spheroids composed solely of fibroblasts, suggesting that these cells are not immune to cytostatic treatment.

Treatment with the 5-fluorouracil: cisplatin 1:1 combination resulted in a strong induction of p21, especially in HCT116 spheroids, while the 1:2 ratio had a weaker effect. From the cellular stress response perspective, the 1:1 combination appears more effective in tumor-only models, whereas the irinotecan: cisplatin 4:1 combination demonstrated broader efficacy, including in fibroblast-containing co-cultures.

Expression of ac-α-tubulin, a marker of stable microtubules often associated with cell survival, followed an inverse trend relative to p21. Combinations that activated p21 generally led to a decrease in ac-α-tubulin levels. This inverse relationship was most apparent with the 5-fluorouracil: cisplatin 1:1 and irinotecan: cisplatin 4:1 treatments, suggesting destabilization of the microtubule network and potential induction of apoptosis. In contrast, the 5-fluorouracil: cisplatin 1:2 combination was associated with a relatively mild stress response, which reflects its lower cytotoxic efficacy.

The data confirm that measurements of p21 and ac-α-tubulin levels provide summary information on the efficacy and mechanisms of drug action. The combination of irinotecan and cisplatin 4:1 was shown to be the most effective across models; the combination of 5-FU: cisplatin 1:1 was highly effective, especially in tumor monocultures, the ratio 1:2 appears to be the least cytotoxic.

No reference protein (loading control) such as β-actin or GAPDH was used in the Western blot analysis. The loaded samples were standardized according to the

quantification of total protein by the BCA method. Therefore, the results are interpreted qualitatively and cannot be used to infer precise differences in the expression of the monitored proteins.

To eliminate the problem of so-called mixed signals, it would be appropriate to separate HCT116 cells from CCD18-Co fibroblasts by flow cytometry, as HCT116 cells are labeled with GFP. Cell separation could lead to improved protein detection and more accurate interpretation of drug effects. This approach would also provide a more detailed view of the interactions between tumor cells and fibroblasts, contributing to a better understanding of the dynamics of cellular responses in spheroid models. Additionally, it would be beneficial to examine other cell cycle or apoptosis-related markers, such as Poly (ADP-ribose) polymerase or B-cell lymphoma 2, to determine the apoptotic stage of the spheroids and to gain a more comprehensive understanding of the cellular response to treatment.

6 Conclusion

Spheroids, as a 3D model mimicking physiological and microtumor environments, have the potential to become a relevant biomedical tool that could be used in clinical laboratories in the future, especially in the increasingly popular field of personalized medicine. This thesis aimed to use established laboratory protocols to create monocultures and cocultures of HCT116 colorectal carcinoma cell lines and CCD18-Co normal colon fibroblast and apply them for various types of testing.

The created spheroids were used in the first part of the work to evaluate the effect of three types of lymphocytes in different concentrations – control untreated lymphocytes, CuET-treated-lymphocytes, and IL-2-treated-lymphocytes – on spheroids after three-day incubation. IL-2-stimulated lymphocytes showed higher cytotoxic activity than CuET-treated lymphocytes, especially in cell lines with functional or partially functional p53. To analyze the effect of lymphocytes, fluorescence microscopy and the ATP measurement method using CellTiter-Glo® 3D were used, which is commonly used to determine the viability of spheroids, but in these experiments, it turned out to be less reliable. Therefore, consistently removing lymphocytes from spheroids before analysis is recommended to achieve more accurate results.

When testing the synergistic effect of drugs, the combination of irinotecan: cisplatin 4:1 proved to be the most effective for inhibiting Ac-α-tubulin and activating p21. Monitoring various cell markers proved to be key for accurately determining the synergistic effect of individual drugs and using cocultures that better simulate the conditions of the real tumor microenvironment.

To achieve more reliable results in experimental laboratory medicine, combining multiple analytical methods that complement each other and provide a more comprehensive view of cellular reactions is important. The use of cocultures with different ratios of tumor and stromal cells, together with a combination of methods, allows for a more detailed assessment of drug efficacy and a better understanding of the mechanisms of cellular response. Spheroids prepared by the agarose-coated plates method have proven to be a suitable model that meets these requirements and provides a reliable platform for future research.

7 References

Ai, M., Budhani, P., Sheng, J., Balasubramanyam, S., Bartkowiak, T., Jaiswal, A. R., Ager, C. R., Haria, D. D., & Curran, M. A. (2015). Tumor hypoxia drives immune suppression and immunotherapy resistance. *Journal for Immunotherapy of Cancer*, *3*(Suppl 2), P392. https://doi.org/10.1186/2051-1426-3-S2-P392

Alzeeb, G., Metges, J.-P., Corcos, L., & Le Jossic-Corcos, C. (2020). Three-Dimensional Culture Systems in Gastric Cancer Research. *Cancers*, *12*(10), 2800. https://doi.org/10.3390/cancers12102800

Astell, K. R., & Sieger, D. (2020). Zebrafish In Vivo Models of Cancer and Metastasis. *Cold Spring Harbor Perspectives in Medicine*, *10*(8), a037077. https://doi.org/10.1101/cshperspect.a037077

Banerjee, D., Singh, Y. P., Datta, P., Ozbolat, V., O'Donnell, A., Yeo, M., & Ozbolat, I. T. (2022). Strategies for 3D bioprinting of spheroids: A comprehensive review. *Biomaterials*, *291*, 121881. https://doi.org/10.1016/j.biomaterials.2022.121881

Bregenzer, M. E., Davis, C., Horst, E. N., Mehta, P., Novak, C. M., Raghavan, S., Snyder, C. S., & Mehta, G. (2019). Physiologic Patient Derived 3D Spheroids for Anti-Neoplastic Drug Screening to Target Cancer Stem Cells. *Journal of Visualized Experiments : JoVE*, *149*, 10.3791/59696. https://doi.org/10.3791/59696

Busse, A., Letsch, A., Fusi, A., Nonnenmacher, A., Stather, D., Ochsenreither, S., Regenbrecht, C. R. A., & Keilholz, U. (2013). Characterization of small spheres derived from various solid tumor cell lines: Are they suitable targets for T cells? *Clinical & Experimental Metastasis*, *30*(6), 781–791. https://doi.org/10.1007/s10585-013-9578-5

Calà, G., Sina, B., De Coppi, P., Giobbe, G. G., & Gerli, M. F. M. (2023). Primary human organoids models: Current progress and key milestones. *Frontiers in Bioengineering and Biotechnology*, *11*. https://doi.org/10.3389/fbioe.2023.1058970

Cao, U. M. N., Zhang, Y., Chen, J., Sayson, D., Pillai, S., & Tran, S. D. (2023). Microfluidic Organ-on-A-chip: A Guide to Biomaterial Choice and Fabrication. *International Journal of Molecular Sciences*, *24*(4), 3232. https://doi.org/10.3390/ijms24043232

Carter, E. P., Roozitalab, R., Gibson, S. V., & Grose, R. P. (2021). Tumour microenvironment 3D-modelling: Simplicity to complexity and back again. *Trends in Cancer*, *7*(11), 1033–1046. https://doi.org/10.1016/j.trecan.2021.06.009

Chatzinikolaidou, M. (2016). Cell spheroids: The new frontiers in *in vitro* models for cancer drug validation. *Drug Discovery Today*, *21*(9), 1553–1560. https://doi.org/10.1016/j.drudis.2016.06.024

Cho, S. K., Moon, H., & Kim, C.-J. (2003). Creating, transporting, cutting, and merging liquid droplets by electrowetting-based actuation for digital microfluidic circuits. *Journal of Microelectromechanical Systems*, *12*(1), 70–80. Journal of Microelectromechanical Systems. https://doi.org/10.1109/JMEMS.2002.807467

Cianciosi, D., Ansary, J., Forbes-Hernandez, T. Y., Regolo, L., Quinzi, D., Gracia Villar, S., Garcia Villena, E., Tutusaus Pifarre, K., Alvarez-Suarez, J. M., Battino, M., & Giampieri, F. (2021). The Molecular Basis of Different Approaches for the Study of Cancer Stem Cells and the Advantages and Disadvantages of a Three-Dimensional Culture. *Molecules*, *26*(9), Article 9. https://doi.org/10.3390/molecules26092615

Courau, T., Bonnereau, J., Chicoteau, J., Bottois, H., Remark, R., Assante Miranda, L., Toubert, A., Blery, M., Aparicio, T., Allez, M., & Le Bourhis, L. (2019). Cocultures of human colorectal tumor spheroids with immune cells reveal the therapeutic potential of MICA/B and NKG2A targeting for cancer treatment. *Journal for Immunotherapy of Cancer*, *7*(1), 74. https://doi.org/10.1186/s40425-019-0553-9

Das, V., Bruzzese, F., Konečný, P., Iannelli, F., Budillon, A., & Hajdúch, M. (2015). Pathophysiologically relevant *in vitro* tumor models for drug screening. *Drug Discovery Today*, *20*(7), 848–855. https://doi.org/10.1016/j.drudis.2015.04.004

Das, V., Fürst, T., Gurská, S., Džubák, P., & Hajdúch, M. (2016). Reproducibility of Uniform Spheroid Formation in 384-Well Plates: The Effect of Medium Evaporation. *Journal of Biomolecular Screening*, *21*(9), 923–930. https://doi.org/10.1177/1087057116651867

Gong, X., Lin, C., Cheng, J., Su, J., Zhao, H., Liu, T., Wen, X., & Zhao, P. (2015). Generation of Multicellular Tumor Spheroids with Microwell-Based Agarose Scaffolds for Drug Testing. *PLOS ONE*, *10*(6), e0130348. https://doi.org/10.1371/journal.pone.0130348

Hickman, J. A., Graeser, R., de Hoogt, R., Vidic, S., Brito, C., Gutekunst, M., van der Kuip, H., & Consortium, I. P. (2014). Three-dimensional models of cancer for pharmacology and cancer cell biology: Capturing tumor complexity in vitro/ex vivo. *Biotechnology Journal*, *9*(9), 1115–1128. https://doi.org/10.1002/biot.201300492

Hu, G., & Li, D. (2007). Three-dimensional modeling of transport of nutrients for multicellular tumor spheroid culture in a microchannel. *Biomedical Microdevices*, *9*(3), 315–323. https://doi.org/10.1007/s10544-006-9035-1

Hughes, C. S., Postovit, L. M., & Lajoie, G. A. (2010). Matrigel: A complex protein mixture required for optimal growth of cell culture. *PROTEOMICS*, *10*(9), 1886–1890. https://doi.org/10.1002/pmic.200900758

Jungreuthmayer, C., Donahue, S. W., Jaasma, M. J., Al-Munajjed, A. A., Zanghellini, J., Kelly, D. J., & O'Brien, F. J. (2009). A comparative study of shear stresses in collagen-glycosaminoglycan and calcium phosphate scaffolds in bone tissue-engineering bioreactors. *Tissue Engineering. Part A*, *15*(5), 1141–1149. https://doi.org/10.1089/ten.tea.2008.0204

Kapałczyńska, M., Kolenda, T., Przybyła, W., Zajączkowska, M., Teresiak, A., Filas, V., Ibbs, M., Bliźniak, R., Łuczewski, Ł., & Lamperska, K. (2016). 2D and 3D cell cultures – a comparison of different types of cancer cell cultures. *Archives of Medical Science : AMS*, *14*(4), 910. https://doi.org/10.5114/aoms.2016.63743

Kijanska, M., & Kelm, J. (2016). In vitro 3D Spheroids and Microtissues: ATP-based Cell Viability and Toxicity Assays. In S. Markossian, A. Grossman, M. Arkin, D. Auld, C. Austin, J. Baell, K. Brimacombe, T. D. Y. Chung, N. P. Coussens, J. L. Dahlin, V. Devanarayan, T. L. Foley, M. Glicksman, K. Gorshkov, J. V. Haas, M. D. Hall, S. Hoare, J. Inglese, P. W. Iversen, … X. Xu (Eds.), *Assay Guidance Manual*. Eli Lilly & Company and the National Center for Advancing Translational Sciences. http://www.ncbi.nlm.nih.gov/books/NBK343426/

Ko, J.-Y., Park, J.-W., Kim, J., & Im, G.-I. (2021). Characterization of adipose-derived stromal/stem cell spheroids versus single-cell suspension in cell survival and arrest of osteoarthritis progression. *Journal of Biomedical Materials Research. Part A*, *109*(6), 869–878. https://doi.org/10.1002/jbm.a.37078

Labuschagne, C. F., Zani, F., & Vousden, K. H. (2018). Control of metabolism by p53 – Cancer and beyond. *Biochimica et Biophysica Acta*, *1870*(1), 32–42. https://doi.org/10.1016/j.bbcan.2018.06.001

Lee, S.-Y., Koo, I.-S., Hwang, H. J., & Lee, D. W. (2023). *In Vitro* three-dimensional (3D) cell culture tools for spheroid and organoid models. *SLAS Discovery*, *28*(4), 119–137. https://doi.org/10.1016/j.slasd.2023.03.006

Li, L., & Yang, X.-J. (2015). Tubulin acetylation: Responsible enzymes, biological functions and human diseases. *Cellular and Molecular Life Sciences: CMLS*, *72*(22), 4237–4255. https://doi.org/10.1007/s00018-015-2000-5

Li, Y., & Kumacheva, E. (2018). Hydrogel microenvironments for cancer spheroid growth and drug screening. *Science Advances*, *4*(4), eaas8998. https://doi.org/10.1126/sciadv.aas8998

Lin, R.-Z., & Chang, H.-Y. (2008). Recent advances in three-dimensional multicellular spheroid culture for biomedical research. *Biotechnology Journal*, *3*(9–10), 1172–1184. https://doi.org/10.1002/biot.200700228

Liu, X., & Hummon, A. B. (2015). Quantitative Determination of Irinotecan and the Metabolite SN-38 by Nanoflow Liquid Chromatography-Tandem Mass Spectrometry in Different Regions of Multicellular Tumor Spheroids. *Journal of the American Society for Mass Spectrometry*, *26*(4), 577–586. https://doi.org/10.1007/s13361-014-1071-0

Malaney, P., Nicosia, S. V., & Davé, V. (2014). One mouse, one patient paradigm: New avatars of personalized cancer therapy. *Cancer Letters*, *344*(1), 1–12. https://doi.org/10.1016/j.canlet.2013.10.010

Miller, R. P., Tadagavadi, R. K., Ramesh, G., & Reeves, W. B. (2010). Mechanisms of Cisplatin Nephrotoxicity. *Toxins*, *2*(11), 2490. https://doi.org/10.3390/toxins2112490

Novak, R., Ingram, M., Marquez, S., Das, D., Delahanty, A., Herland, A., Maoz, B. M., Jeanty, S. S. F., Somayaji, M. R., Burt, M., Calamari, E., Chalkiadaki, A., Cho, A., Choe, Y., Chou, D. B., Cronce, M., Dauth, S., Divic, T., Fernandez-Alcon, J., … Ingber, D. E. (2020). Robotic fluidic coupling and interrogation of multiple vascularized organ chips. *Nature Biomedical Engineering*, *4*(4), 407–420. https://doi.org/10.1038/s41551-019-0497-x

Ortiz-Otero, N., Clinch, A. B., Hope, J., Wang, W., Reinhart-King, C. A., & King, M. R. (2020). Cancer associated fibroblasts confer shear resistance to circulating tumor cells during prostate cancer metastatic progression. *Oncotarget*, *11*(12), 1037–1050. https://doi.org/10.18632/oncotarget.27510

Oshimi, K., Oshimi, Y., Akutsu, M., Takei, Y., Saito, H., Okada, M., & Mizoguchi, H. (1986). Cytotoxicity of Interleukin 2-Activated Lymphocytes for Leukemia and Lymphoma Cells. *Blood*, *68*(4), 938–948. https://doi.org/10.1182/blood.V68.4.938.938

Pokorná, V. (2022). *Diethyldithiocarbamate Copper (CuEt) effect on lymphocyte activation and antitumor responses* [Bachelor theses]. Univerzita Palackého v Olomouci, Přírodovědecká fakulta.

Rasouli, M., Safari, F., Kanani, M. H., & Ahvati, H. (2024). Principles of Hanging Drop Method (Spheroid Formation) in Cell Culture. *Methods in Molecular Biology (Clifton, N.J.)*. https://doi.org/10.1007/7651_2024_527

Sakalem, M., Sibio, M., Costa, F., & Oliveira, M. (2020). *Historical evolution of spheroids and organoids, and possibilities of use in life sciences and medicine*. https://doi.org/10.22541/au.159430472.23281090

Salinas-Vera, Y. M., Valdés, J., Pérez-Navarro, Y., Mandujano-Lazaro, G., Marchat, L. A., Ramos-Payán, R., Nuñez-Olvera, S. I., Pérez-Plascencia, C., & López-Camarillo, C. (2022). Three-Dimensional 3D Culture Models in Gynecological and Breast Cancer Research. *Frontiers in Oncology*, *12*, 826113. https://doi.org/10.3389/fonc.2022.826113

Sato, T., Stange, D. E., Ferrante, M., Vries, R. G. J., van Es, J. H., van den Brink, S., van Houdt, W. J., Pronk, A., van Gorp, J., Siersema, P. D., & Clevers, H. (2011). Long-term Expansion of Epithelial Organoids From Human Colon, Adenoma, Adenocarcinoma, and Barrett's Epithelium. *Gastroenterology*, *141*(5), 1762–1772. https://doi.org/10.1053/j.gastro.2011.07.050

Suenaga, H., Furukawa, K. S., Suzuki, Y., Takato, T., & Ushida, T. (2015). Bone regeneration in calvarial defects in a rat model by implantation of human bone marrow-derived mesenchymal stromal cell spheroids. *Journal of Materials Science. Materials in Medicine*, *26*(11), 254. https://doi.org/10.1007/s10856-015-5591-3

Suryaprakash, S., Lao, Y.-H., Cho, H.-Y., Li, M., Ji, H. Y., Shao, D., Hu, H., Quek, C. H., Huang, D., Mintz, R. L., Bagó, J. R., Hingtgen, S. D., Lee, K.-B., & Leong, K. W. (2019). Engineered Mesenchymal Stem Cell/Nanomedicine Spheroid as an Active Drug Delivery Platform for Combinational Glioblastoma Therapy. *Nano Letters*, *19*(3), 1701–1705. https://doi.org/10.1021/acs.nanolett.8b04697

Sutherland, R. M. (1988). Cell and Environment Interactions in Tumor Microregions: The Multicell Spheroid Model. *Science*, *240*(4849), 177–184. https://doi.org/10.1126/science.2451290

Tevlek, A., Kecili, S., Ozcelik, O. S., Kulah, H., & Tekin, H. C. (2023). Spheroid Engineering in Microfluidic Devices. *ACS Omega*, *8*(4), 3630. https://doi.org/10.1021/acsomega.2c06052

Tung, Y.-C., Hsiao, A. Y., Allen, S. G., Torisawa, Y., Ho, M., & Takayama, S. (2011). High-throughput 3D spheroid culture and drug testing using a 384 hanging drop array. *The Analyst*, *136*(3), 473–478. https://doi.org/10.1039/c0an00609b

Vrablíková, B. (2022). *Analysis of cancer drug combination using 3D mono- and co-cultures of colorectal cell lines* [Diplomová práce, Univerzita Palackého v Olomouci, Přírodovědecká fakulta]. https://theses.cz/id/mi6rm0/Vrablikova_DP.pdf?info

Wang, J., Chu, R., Ni, N., & Nan, G. (2020). The effect of Matrigel as scaffold material for neural stem cell transplantation for treating spinal cord injury. *Scientific Reports*, *10*(1), 2576. https://doi.org/10.1038/s41598-020-59148-3

Yao, T., & Asayama, Y. (2017). Animal-cell culture media: History, characteristics, and current issues. *Reproductive Medicine and Biology*, *16*(2), 99–117. https://doi.org/10.1002/rmb2.12024

Yu, L., Chen, M. C. W., & Cheung, K. C. (2010). Droplet-based microfluidic system for multicellular tumor spheroid formation and anticancer drug testing. *Lab on a Chip*, *10*(18), 2424–2432. https://doi.org/10.1039/c004590j

Yun, C., Kim, S. H., Kim, K. M., Yang, M. H., Byun, M. R., Kim, J.-H., Kwon, D., Pham, H. T. M., Kim, H.-S., Kim, J.-H., & Jung, Y.-S. (2024). Advantages of Using 3D Spheroid Culture Systems in Toxicological and Pharmacological Assessment for Osteogenesis Research. *International Journal of Molecular Sciences*, *25*(5), 2512. https://doi.org/10.3390/ijms25052512

Zhang, K., Yan, S., Li, G., Cui, L., & Yin, J. (2015). In-situ birth of MSCs multicellular spheroids in poly(l-glutamic acid)/chitosan scaffold for hyaline-like cartilage regeneration. *Biomaterials*, *71*, 24–34. https://doi.org/10.1016/j.biomaterials.2015.08.037

Zhang, N., Yin, Y., Xu, S.-J., & Chen, W.-S. (2008). 5-Fluorouracil: Mechanisms of Resistance and Reversal Strategies. *Molecules*, *13*(8), 1551. https://doi.org/10.3390/molecules13081551

Zhu, Y., Kang, E., Wilson, M., Basso, T., Chen, E., Yu, Y., & Li, Y.-R. (2022). 3D Tumor Spheroid and Organoid to Model Tumor Microenvironment for Cancer Immunotherapy. *Organoids*, *1*(2), Article 2. https://doi.org/10.3390/organoids1020012

8 List of symbols and abbreviations

Ac-α-tubulin	Acetyl-α-tubulin
BCA	Bicinchoninic acid
CDK	Cyclin-dependent kinase
CuET	Copper diethyldithiocarbamate
DMEM	Dulbecco's Modified Eagle Medium
EDTA	Ethylenediaminetetraacetic acid
ECM	Extracellular matrix
FAK	Focal adhesion kinase
G	G - force
HLA	Human leukocyte antigen
IL-2	Interleukin 2
MSC	Mesenchymal stem cells
EMEM	Minimum Essential Medium Eagle
MSC	Multicellular spheroids
nLC-MS/MS	Nanoflow liquid chromatography-tandem mass spectrometry
NK	Natural killer
OOC	Organ-on-chip
PBS	Phosphate buffer
TBS-T	Tris-buffered saline with Tween 20
RT	Room temperature
SDS-PAGE	Sodium dodecyl sulfate–polyacrylamide gel electrophoresis